DOI: 10.1590/2317-4889201620150012

ARTICLE

U-Pb zircon ages of rocks from the Amazonas Territory of Colombia and their bearing on the tectonic history of the NW sector of the Amazonian Craton

Idades U-Pb em zircão de rochas do Território Amazonas da Colômbia e sua relevância para a história tectônica do setor NW do Cráton Amazônico

Umberto Giuseppe Cordani[1]*, Kei Sato[1], Walter Sproessner[1], Fabiana Santos Fernandes[1]

ABSTRACT: Here we report the results of several U-Pb zircon ages, made to generate an integrated history for the Rio Negro-Juruena tectonic province, for the northwestern part of the Amazonian Craton. This region comprises granitoid rocks, described as calc-alkaline syntectonic gneisses, granites and migmatites, affected by medium level amphibolite facies metamorphism. The new measurements, with the available Rb-Sr and K-Ar ages, indicate the formation of these rocks within a series of essentially juvenile magmatic arcs, that are closely related with subduction. Sm-Nd analyses indicate that all samples, regardless of their zircon ages, yielded T_{DM} model ages roughly between 1.9 and 2.2 Ga, suggesting the absence of a much older source material. In the northeastern part (areas of Puerto Inírida and San Carlos), the Atabapo belt comprises rocks formed within a period of about 60 Ma, from 1800 to 1740 Ma. In the southwestern region, including the towns of Mitú and Iauaretê, the granitoids formed in the Vaupés belt between 1580 and 1520 Ma. Finally, the available K-Ar measurements indicate the onset of the Nickerie-K'Mudku intraplate heating event, with temperature above 300ºC within the entire region at 1200 – 1300 Ma.

KEYWORDS: Amazonian Craton; Rio Negro-Juruena province; geochronology; zircon ages; tectonic history.

RESUMO: *Este trabalho inclui diversas idades U-Pb SHRIMP e LA_ICP-MS em zircão, produzidas para contribuir com o conhecimento da história geológica da província tectônica Rio Negro-Juruena na parte noroeste do Craton Amazônico. A região é constituída por rochas granitoides, descritas como gnaisses, granitos e migmatitos cálcio-alcalinos, afetadas por metamorfismo de fácies anfibolito, em nível crustal médio. As novas datações, com as idades K-Ar e Rb-Sr previamente existentes, indicam a formação dessas rochas numa série de arcos magmáticos essencialmente juvenis, associados a processos de subducção. A sistemática Sm-Nd indica que todas as amostras analisadas, quaisquer que sejam as suas idades, apresentam idades modelo T_{DM} entre 1,9 e 2,2 Ga, sugerindo ausência de material crustal mais antigo. Na parte nordeste (áreas de Puerto Inírida e San Carlos), a Faixa Atabapo inclui rochas formadas num período de 60 Ma, entre 1800 e 1740 Ma. Na parte sudoeste, que inclui as vilas de Mitú e Iauaretê, os granitoides foram formados entre 1580 e 1520 Ma na Faixa Vaupés. Finalmente, as idades K-Ar disponíveis indicam o advento do importante aquecimento intraplaca cobrindo a região inteira, acima de 300ºC, denominado Nickerie-K'Mudku, com ca. 1200 – 1300 Ma.*

PALAVRAS-CHAVE: *Craton Amazônico; Província Rio Negro-Juruena; Geocronolgia; Idades em zircão; História tectônica.*

[1]Institute of Geosciences, Universidade de São Paulo - USP, São Paulo (SP), Brazil. *E-mails: ucordani@usp.br, keisato@usp.br, wmsproes@usp.br, fabianaf00@yahoo.com.br*

*Corresponding author.

Manuscript ID: 20150012. **Received in:** 06/29/2015. **Approved in:** 10/08/2015.

INTRODUCTION

A first attempt towards a geochronological reconnaissance study of the Amazonian Craton was made in the late 1970's (Cordani *et al.* 1979), after comprehensive geological mapping through the RADAM program of the Brazilian government. In contrast from the previous fixistic tectonic models for that cratonic area, these authors adopted a mobilistic interpretation. Some proterozoic tectonic provinces were envisaged, growing successively around an ancient nucleus located in the central part of the craton. One of them, including the Amazonian region of eastern Colombia, SW Venezuela and NW Brazil, was named Rio Negro-Juruena tectonic province.

At the time of the initial work, only Rb-Sr and K-Ar ages were available. Cordani *et al.* (1979) reported ages between 1700 and 1500 Ma for the tectonic events within that province. A later increase of available rock ages in Amazonia permitted marked progress in understanding the region (see e.g, comprehensive reviews by Teixeira *et al.* (1989), Tassinari (1996), Tassinari and Macambira (1999) and Cordani *et al*. (2000).

With the increasing use of U-Pb zircon ages in recent years, some alternative interpretations for the tectonic evolution of the Amazonian Craton were presented (e.g. Santos *et al.* 2000, Santos 2003, Cordani and Teixeira 2007). Boundaries of the tectonic domains were altered, and names were changed, but the mobilistic frame was always maintained. Based on Nd isotopic work, Cordani and Teixeira (2007) suggested that the tectonic evolution of the SW half of the Amazonian Craton was accretionary. They proposed that the craton grew by the stacking of successive magmatic arcs originating from subduction zones, from 2000 to1500 Ma. Within the Rio Negro-Juruena province, unequivocal evidence of continental material older than 2000 Ma has not been found.

Figure 1 illustrates the interpretation given by Cordani *et al.* (2000), with the location of the study area. The first geochronological ages in that region were determined by Pinson *et al.* (1962), who dated the alkaline rocks of São José del Guaviare by the K-Ar method, back to an ordovician age (about 480 Ma). During the 1970's and the 1980's, the Geological Survey of Colombia, INGEOMINAS, made an extensive reconnaissance geological mapping of the country (PRORADAM 1979). Priem *et al.* (1982) performed a relevant geochronological study of that area, primarily using Rb-Sr and K-Ar methods. Around the same time, important reconnaissance works were carried out in Brazil and Venezuela by the respective geological surveys, to assess the potential of the region for mineral exploration.

Our original focus in this work was the poorly known region of the Amazonas Territory of Colombia, located in the NW part of the Rio Negro-Juruena Province of Cordani *et al.* (1979). We later enlarged the area of interest to involve large parts of SW Venezuela and NW Brazil. In these countries, a few important geochronological works by Fernandes *et al.* (1976), Pinheiro *et al*. (1976), Gaudette and Olszewski (1985), and Barrios *et al.* (1985 and 1986) made several age determinations for the existent governmental mapping projects. Our consolidated study area (Fig. 2) includes the international boundaries of Colombia with Venezuela and Brazil. The terrain of the entire territory was completely shaped by erosion, and the present land surface is a widespread peneplain. Granitic and gneissic rocks, deformed or not, and frequently migmatitic, are largely predominant. In a general way, these regional rocks were formed by tectono-magmatic and metamorphic processes related to medium-grade metamorphic environments. Supracrustal rocks and intraplate volcanic-sedimentary sequences occur in restricted areas.

During the 1980's, Priem *et al.* (1982) and Gaudette and Olszewski (1985) produced a few U-Pb zircon analyses, using conventional TIMS studies. Important geochronological papers were later produced, including work by Tassinari *et al.* (1996), using SHRIMP, and by Sato and Tassinari (1997), using Sm-Nd model ages. Tassinari (1996) prepared a complete synthesis of all available geochronological ages in the Brazilian territory. In the last 10 to 20 years, additional U-Pb zircon work has been performed, such as studies by Santos *et al.* (2000), Santos (2003), Almeida (2006), and, more recently, Ibañez *et al.* (2011), who presented a few U-Pb zircon determinations by LA-ICP-MS.

The aim of the present work was to produce a tentative integrated picture of the tectonic evolution of the NW part of the Amazonian Craton. Following the analyses of about 20 samples of granitoid rocks from the INGEOMINAS collection, we report the results of geochronological and isotopic measurements using accurate U-Pb zircon ages, measured by the SHRIMP or LA-ICP-MS methods. Despite the reasonable amount of available geochronological data, this project remains a very preliminary reconnaissance work, because the covered basement area exceeds 200,000 km^2 and only around 30 precise U-Pb zircon ages exist. This work includes the results of several new Sm-Nd isotopic measurements and some new Rb-Sr analyses which were included in the available isochron diagrams constructed from works of Priem *et al.* (1982) and others. Our regional interpretations consider all available geochronological controls, by K-Ar and Rb-Sr methods. As more than 100 ages by Rb-Sr dating are available for the study area, we tried

to select the most significant ages in terms of interpretative results. Figure 3 shows the location of 97 rock samples with Rb-Sr determinations. Their ages are described in a series of Rb-Sr isochron diagrams (Fig. 9) and will be properly discussed later. Overall, these data have helped us to obtain a suitable perspective for interpreting the tectonic history of the region.

ANALYTICAL METHODS

All K-Ar and most Rb-Sr dates considered in this work were obtained during the 1970's and 1980's from laboratories in Amsterdam (Priem *et al.* 1982) and São Paulo (Barrios *et al.* 1985, Fernandes *et al.* 1976, Pinheiro *et al.* 1976). Analytical procedures can be found in the indicated

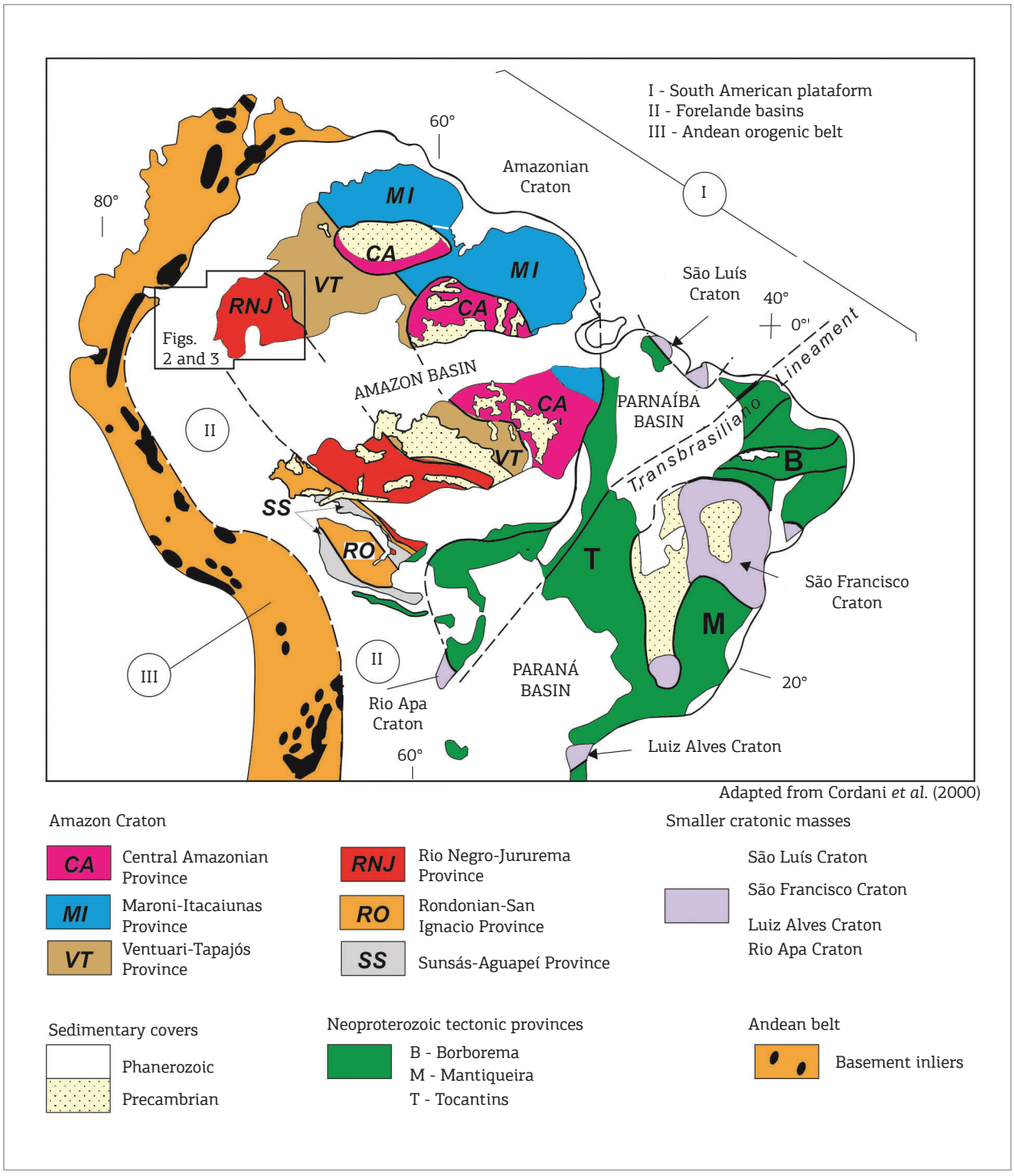

Figure 1. Tectonic provinces of the Amazonian Craton, with location of the study area.

references. Andrade-Santos (2010) obtained 10 additional Rb-Sr whole-rock measurements at the São Paulo laboratory (CPGeo-USP). Analytical procedures are the same as indicated by Tassinari (1996). The instrument used was a Finnegan-MAT 262, with five Faraday collectors operated in a static way. Table 1 provides the analytical data for the 97 Rb-Sr measurements considered in this work.

A few Sm-Nd measurements, reported by Sato and Tassinari (1997), were produced at the CPGeo-USP, by using the same instrument used for the Rb-Sr measurements. Sixteen measurements, reported by Andrade-Santos (2010), were later made in the same laboratory by employing ^{149}Sm and ^{150}Nd spikes, as well as elemental separation by AG50WX8 and LN Spec resins (Sato *et al.* 1995). All Sm-Nd analyses available for the studied area are included in Table 2.

Several U-Pb zircon ages, obtained by TIMS, were available from the works of Priem *et al.* (1982) and Gaudette and Olszewski (1985). Santos *et al.* (2000) and Ibañez *et al.* (2011) produced additional U-Pb ages by Pb evaporation, SHRIMP or LA-ICP-MS. All them are displayed in Table 3. Analytical procedures are provided in the respective references.

For U-Pb dating in this work, zircon grains were extracted by standard crushing, milling, sieving (0.150 – 0.063 μm), Wilfley table, Franz and heavy liquid techniques. Extracted grains were set in an epoxy disk and polished to reveal half sections. Reflected, transmitted and cathodoluminescence (CL) images were obtained by SEM and XMAX CL detectors.

Eight U-Pb dates were obtained by SHRIMP II at the GeoLab-IGc-USP (Sato *et al.* 2014). Mounts were gold-coated, and dating was performed with the standard Temora2 for age reference and SL13 for uranium composition. Acquisition was obtained by following the procedure described in Williams (1998). Individual ages were determined from six successive MS scans. Correction for common Pb was made based on the measured ^{204}Pb. The typical error component for ^{206}Pb/^{238}U ratios is less than 2%. Data were reduced by using SQUID 1.06. Concordia diagrams were plotted with ISOPLOT 4 (Ludwig 2009). Analytical results are included in Annex I.

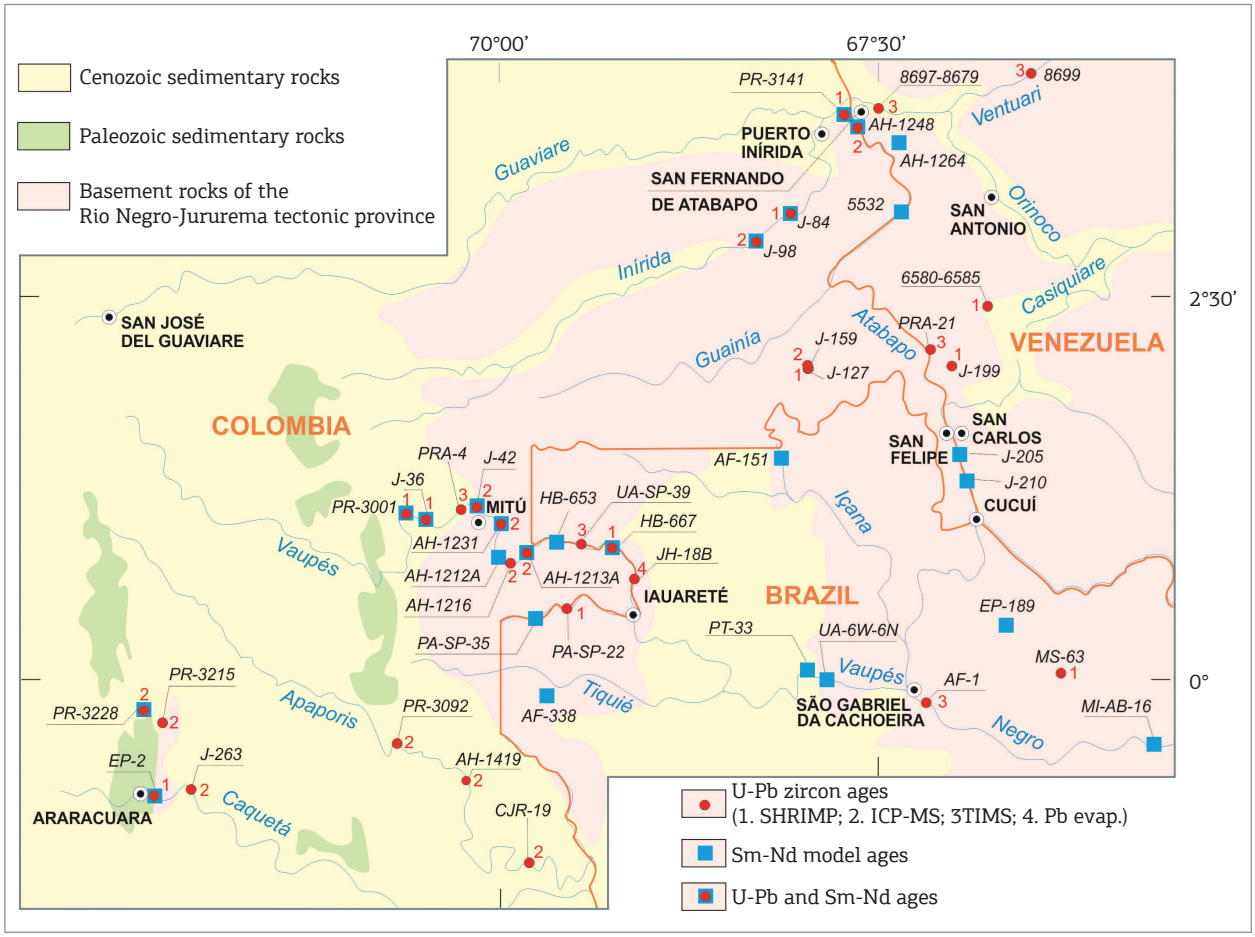

Figure 2. NW Corner of the Amazonian Craton. Location of samples analysed by the U-Pb and Sm-Nd methods.

Seven U-Pb zircon ages were determined by a Neptune ICP-MS instrument coupled with an excimer laser ablation system. Khan titanite standard was utilized for mass bias correction and the GJ standard was utilized for zircon. Residual common Pb was corrected by using the terrestrial composition reported by Stacey and Kramer (1975). Analytical results are included in Annex II. However, these U-Pb LA-ICP-MS analyses were done in 2009, at the very beginning of the use of our instrument, when we were still dealing with the calibration of it. Now we do not have the complete knowledge of the analytical conditions of that time, when the software was set up for detrital zircon and was not optimized for crystallization ages. The Concordia diagrams of Fig. 7 are rather odd. Several measurements indicate reverse discordance, which may have been caused by inadequate adjustment of the detectors, or to some inadequacy of the ^{204}Pb correction, when the 204 peak may have been not properly stabilized, or perhaps to some Hg interference not detected. We are keeping the diagrams as they were produced in 2009, and the rather imprecise calculated ages are only used in this paper as indicators for the regional interpretation.

NEW U-PB ZIRCON AGES

Figure 2 illustrates the study area and location of samples with U-Pb zircon ages, 15 of which were produced in this work. Cathodoluminescence (CL) images of some selected zircons dated by SHRIMP are shown in Figs. 4A to 4H. The resulting Concordia diagrams are provided in Figs. 5A to 5H.

J-36 – Muscovite-chlorite paragneiss – Vaupés River, near Mitú, Colombia

Sample J-36 is a fine-grained muscovite-chlorite paragneiss, with a granolepidoblastic structure and centimetric porphyroblasts of plagioclase. Zircons from this rock range in size from 70 to 220 μm and exhibit length to width ratios from 2:1 to 3:1. CL images reveal oscillatory zoning

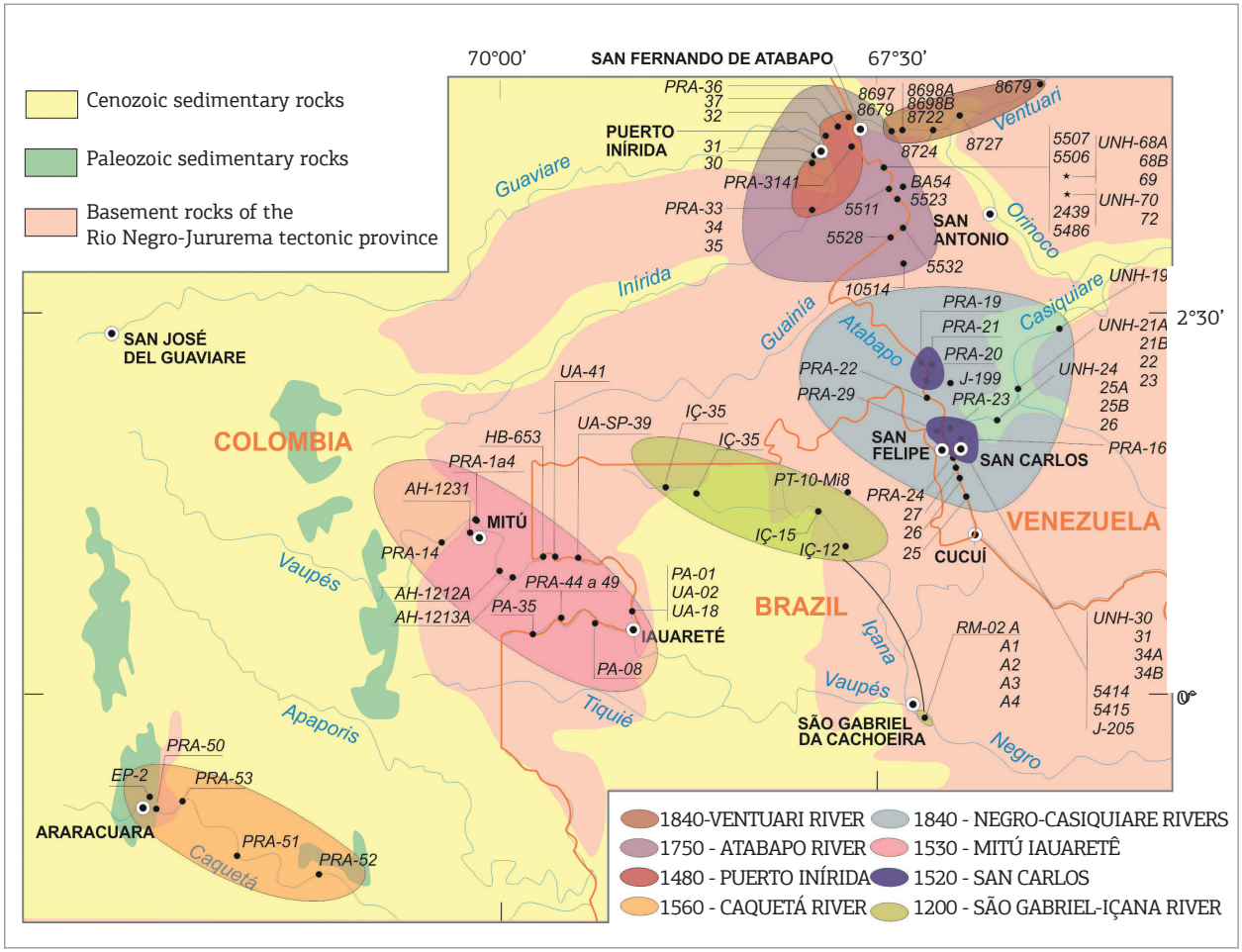

Figure 3. Location of samples analysed by the Rb-Sr method.

Table 1. Rb-Sr analytical data for the rock samples included in Fig. 3.

Sample	Location	Rb, ppm	Sr, ppm	$^{87}Rb/^{86}Sr$	$^{87}Sr/^{86}Sr$	References
San Carlos						
UNH30	San Carlos, Venezuela	411	83	14.870	1.03800	1
UNH31	San Carlos, Venezuela	396	87.5	13.470	1.00700	1
UNH34A	San Carlos, Venezuela	264	349	2.195	0.75190	1
UNH34B	San Carlos, Venezuela	254	324	2.277	0.75630	1
5414	San Carlos, Venezuela	261	323	2.350	0.75570	2
5415	San Carlos, Venezuela	269	229	3.420	0.77790	2
J-205	San Felipe, Colombia	227.5	286.7	2.307	0.75650	6
PRA-16	San Felipe, Colombia	348	99.3	10.340	0.91973	3
PRA-20	Rio Negro,Colombia	279	93.5	8.780	0.89308	3
PRA-21	Rio Negro,Colombia	293	177	4.850	0.81300	3
PRA-23	Rio Negro,Colombia	217	356	1.770	0.74388	3
PRA-29	San Felipe, Colombia	183	224	2.380	0.75699	3
Puerto Inírida						
PRA-30	Puerto Inírida, Colombia	351	316	3.050	0.76941	3
PRA-32	Puerto Inírida, Colombia	372	253	4.310	0.79862	3
PRA-33	Puerto Inírida, Colombia	376	126	8.790	0.89272	3
PRA-34	Puerto Inírida, Colombia	370	134	8.140	0.87994	3
PRA-35	Puerto Inírida, Colombia	363	144	7.440	0.86444	3
PRA-37	Puerto Inírida, Colombia	266	359	2.150	0.75248	3
PR-3141	Puerto Inírida, Colombia	389.2	180.5	6.322	0.83872	6
São Gabriel + Içana River						
RM-O2 A	São Gabriel da Cachoeira, Brazil	252.1	232.9	3.156	0.77730	4
RM-O2 A1	São Gabriel da Cachoeira, Brazil	258.3	205.4	3.669	0.78420	4
RM-02 A2	São Gabriel da Cachoeira, Brazil	288.9	198.6	4.249	0.79700	4
RM-02 A3	São Gabriel da Cachoeira, Brazil	289.8	214.3	3.947	0.78800	4
RM-O2 A4	São Gabriel da Cachoeira, Brazil	268.5	222.1	3.542	0.78240	4
IÇ-12	Içana river, Brazil	290.8	167.9	5.064	0.80620	4
IÇ-15	Içana river, Brazil	308.3	119.3	7.591	0.85500	4
IÇ-29	Içana river, Brazil	340.5	100.3	10.013	0.89660	4
IÇ-35	Içana river, Brazil	344.5	98.5	10.319	0.89970	4
PT-10-Mi8	Içana river, Brazil	659.4	168.5	11.565	0.91700	4
Negro River						
PRA-22	Guainia river, Colombia	215	156	3.988	0.80576	3
PRA-24	San Felipe, Colombia	303	106	8.271	0.91560	3

Continue...

Table 1. Continuation.

Sample	Location	Rb, ppm	Sr, ppm	$^{87}Rb/^{86}Sr$	$^{87}Sr/^{86}Sr$	References
PRA-25	Negro river, Colombia	211	172	3.549	0.79603	3
PRA-26	Negro river, Colombia	245	165	4.296	0.81348	3
PRA-27	Negro river, Colombia	260	163	4.615	0.82460	3
J-199	Negro river, Colombia	406.8	154.7	7.611	0.89623	6
PRA-19	Negro river, Colombia	249	146	5.000	0.82784	3
UNH-19	Casiquiare river, Venezuela	165	150	3.225	0.78860	1
UNH-21A	Casiquiare river, Venezuela	279	71.8	11.570	0.99060	1
UNH-21B	Casiquiare river, Venezuela	271	70.2	11.500	0.99860	1
UNH-22	Casiquiare river, Venezuela	216	231	2.729	0.76970	1
UNH-23	Casiquiare river, Venezuela	226	148	4.473	0.82060	1
UNH-24	Casiquiare river, Venezuela	132	437	0.877	0.72660	1
UNH-25A	Casiquiare river, Venezuela	179	344	1.509	0.73920	1
UNH-25B	Casiquiare river, Venezuela	191	342	1.622	0.74270	1
UNH-26	Casiquiare river, Venezuela	149	503	0.861	0.72470	1
Caquetá River						
PRA-51	Caquetá river, Colombia	505	105	14.410	1.01970	3
PRA-52	Caquetá river, Colombia	268	131	6.030	0.83422	3
PRA-53	Caquetá river, Colombia	406	68.4	17.850	1.09820	3
PRA-50	Araracuara, Colombia	327	86.2	11.270	0.97398	3
EP-2	Araracuara, Colombia	274.7	60.9	13.446	1.00664	6
Rio Atabapo						
PRA-31	Inírida river, Colombia	211	221	2.790	0.77596	3
PRA-36	Inírida river, Colombia	247	180	4.010	0.80642	3
UNH-68 A	Atabapo river, Venezuela	239	151	4.631	0.82730	1
UNH-68 B	Atabapo river, Venezuela	252	149	4.952	0.83170	1
UNH-69	Atabapo river, Venezuela	281	160	5.133	0.83610	1
UNH-70	Atabapo river, Venezuela	234	210	3.251	0.78880	1
UNH-72	Atabapo river, Venezuela	242	173	4.076	0.81010	1
5511	Atabapo river, Venezuela	222	166	3.920	0.79750	2
5523	Atabapo river, Venezuela	248	164	4.440	0.81900	2
5480	Atabapo river, Venezuela	287	135	6.240	0.86300	2
5506	Atabapo river, Venezuela	280	153	5.370	0.84300	2
5507	Atabapo river, Venezuela	326	108	8.980	0.93570	2
5528	Atabapo river, Venezuela	264	156	4.970	0.83410	2
5532	Atabapo river, Venezuela	179	179	3.900	0.80610	2

Continue...

Table 1. Continuation.

Sample	Location	Rb, ppm	Sr, ppm	$^{87}Rb/^{86}Sr$	$^{87}Sr/^{86}Sr$	References
2439	Atabapo river, Venezuela	241	191	3.680	0.79720	2
10514	Atabapo river, Venezuela	190	211	2.630	0.77870	5
BA54	Atabapo river, Venezuela	273	148	5.430	0.84350	5
Região Mitú – Iauaretê						
PRA-1	Mitú, Colombia	280	151	5.410	0.82390	3
PRA-2	Mitú, Colombia	273	153	5.220	0.82820	3
PRA-3	Mitú, Colombia	312	111	8.290	0.88956	3
PRA-4	Mitú, Colombia	238	100	6.970	0.86076	3
PRA-14	Vaupés river, Colombia	327	117	8.260	0.88758	3
PRA-44 A	Papuri river, Colombia	166	307	1.570	0.74145	3
PRA-44 B	Papuri river, Colombia	174	301	1.670	0.74335	3
PRA-45	Papuri river, Colombia	153	353	1.260	0.73393	3
PRA-46	Papuri river, Colombia	184	291	1.840	0.74659	3
PRA-47	Papuri river, Colombia	166	321	1.500	0.73938	3
PRA-48	Papuri river, Colombia	174	292	1.730	0.74455	3
PRA-49	Papuri river, Colombia	201	324	1.800	0.74629	3
PA-01	Iauaretê, Brazil	336.6	156.8	6.301	0.84740	4
PA-08	Papuri river, Brazil	112.6	451.6	0.723	0.72210	4
PA-35	Papuri river, Brazil	62.4	386.8	0.467	0.71560	4
UA-02	Iauaretê, Brazil	384	189.9	5.929	0.83670	4
UA-18	Iauaretê, Brazil	214.4	250.6	2.490	0.75910	4
UA-39	Uaupés river, Brazil	171.5	515.3	0.965	0.72650	4
UA-41	Uaupés river, Brazil	162.2	341.6	1.379	0.73680	4
AH-1212 A	Vaupes river, Colombia	161.8	76.7	6.181	0.83691	6
AH-1213 A	Vaupes river, Colombia	115.9	159.2	2.118	0.75528	6
AH-1231	Mitú, Colombia	334.2	223	4.376	0.79724	6
HB-653	Vaupes river, Colombia	78.1	220.4	1.028	0.73392	6
Ventuari River						
8697	Minicia, Venezuela	132	169	2.272	0.76090	1
8698A	Ventuari river, Venezuela	150	339	1.287	0.73740	1
8698B	Ventuari river, Venezuela	128	229	1.629	0.74340	1
8722	Ventuari river, Venezuela	162	298	1.581	0.74580	1
8724	Ventuari river, Venezuela	116	504	0.669	0.71980	1
8727	Ventuari river, Venezuela	161	296	1.576	0.74180	1
8699	Macabana, Venezuela	300	198	4.451	0.82150	1

References: 1 – Gaudette, Olszewski Jr. 1985; 2 – Barrios *et al.* 1985; 3 – Priem *et al.* 1982; 4 – Fernandes *et al.* 1976; 5 – Barrios 1983; 6 – This work.

(e.g. zircon 10.1 of Fig. 4A). This rock is a paragneiss; however, only 13 zircons were dated, which is too few to analyse the statistical significance of the detrital zircons distribution. The Concordia diagram (Fig. 5A) shows that many of the analytical points are discordant. Only 5 of them are relatively close to the Concordia, with ages between 1800 and 1000 Ma. Zircons 4.1 (6/38 age of 2094 ± 17 Ma) and 13.1 (6/38 age of 2089 ± 16 Ma) indicate the possible existence of much older sources.

J-127 – Tonalitic orthogneiss – Caño Naquen, Guainia River, Colombia

Sample J-127 is a coarse-grained tonalitic orthogneiss with biotite, hornblende and some muscovite. Zircons

Table 2. Sm-Nd analytical data.

Field number	Material	Sm (ppm)	Nd (ppm)	$^{147}Sm/^{144}Nd$	$^{143}Nd/^{144}Nd$	$e_{(0)}$	$f_{Sm/Nd}$	T_{DM} (Ma)	$e_{(TDM)}$	T1 (MA)	$e_{(T1)}$
AH-1264	Monzogranite	7.704	42.131	0.1106	0.511563	-20.97	-0.44	2192.4	3.11	1780.0*	-1.42
AH-1212A	Monzogranite	19.584	138.895	0.0853	0.511403	-24.09	-0.57	1947.7	3.59	1580.0*	-1.63
AH-1248	Paragneiss	5.334	31.829	0.1013	0.511512	-21.96	-0.48	2079.7	3.33	NA	NA
PR-3001	Orthogneiss	8.575	45.665	0.1136	0.511702	-18.26	-0.42	2042.7	3.41	1769.0	0.50
AH-1213A	Orthogneiss	10.780	55.720	0.1170	0.511710	-18.10	-0.41	2103.7	3.29	1736.0	-0.45
AH-1231	Monzogranite	11.734	71.474	0.0993	0.511620	-19.86	-0.50	1895.8	3.70	1510.0	-1.09
PR-3141	Orthogneiss	10.552	71.397	0.0894	0.511367	-24.79	-0.55	2057.5	3.37	1501.0	-4.24
HB-653	Orthogneiss	6.444	33.999	0.1146	0.511692	-18.45	-0.42	2080.6	3.33	1780.0*	0.18
HB-667	Monzogranite	23.987	112.702	0.1287	0.511826	-15.84	-0.35	2186.8	3.13	1779.0	-0.41
EP-2	Orthogneiss	7.856	46.858	0.1014	0.511559	-21.05	-0.48	2015.7	3.46	1721.0	-0.12
PR-3228	Paragneiss	6.057	29.463	0.1243	0.511840	-15.57	-0.37	2052.8	3.39	NA	NA
J-36	Paragneiss	10.853	54.083	0.1213	0.511762	-17.09	-0.38	2117.1	3.26	NA	NA
J-42	Paragneiss	6.054	30.486	0.1201	0.511719	-17.93	-0.39	2159.6	3.18	NA	NA
J-84	Monzogranite	16.318	83.315	0.1184	0.511700	-18.30	-0.40	2152.6	3.19	1507.0	-3.25
J-98	Monzogranite	14.585	83.979	0.1050	0.511534	-21.54	-0.47	2119.8	3.25	1752.0	-1.05
J-210	Granodiorite	7.832	41.791	0.1133	0.511566	-20.91	-0.42	2249.2	3.01	1770.0*	-2.09
PT33ASU	Monzogranite	14.973	86.604	0.1045	0.511624	-19.78	-0.47	1982.7	3.53	1520.0*	-1.91
PT33ASW	Monzogranite	17.167	93.060	0.1116	0.511671	-18.86	-0.43	2049.2	3.39	1520.0*	-2.35
UA-6W	Monzogranite	14.688	81.796	0.1086	0.511651	-19.25	-0.45	2020.1	3.45	1520.0*	-2.17
5532	Tonalite	11.397	69.104	0.0997	0.511415	-23.86	-0.49	2182.1	3.13	1860.0*	-0.85
PA-35	Tonalite	2.087	9.526	0.1325	0.511771	-16.91	-0.33	2398.5	2.73	1830.0*	-1.92
MI-AB-16	Granodiorite	2.675	21.485	0.0753	0.511123	-29.55	-0.62	2118.4	3.25	1520.0*	-6.01
J-127	Orthogneiss	5.940	31.256	0.1149	0.511660	-19.08	-0.42	2137.6	3.22	1775.0	-0.56
J-159	Tonalite	8.590	42.302	0.1228	0.511790	-16.54	-0.38	2103.5	3.29	1770.0	0.14
J-205	Tonalite	16.576	89.887	0.1115	0.511589	-20.46	-0.43	2173.2	3.15	1740.0*	-1.56
J-199	Orthogneiss	11.379	65.677	0.1048	0.511532	-21.57	-0.47	2117.7	3.26	1796.0	-0.51
AF-151	Not available							2029.0			
AF-338	Not available							1937.0			
EP-189	Not available							1900.0			

*T1: estimated age; NA: Not applicable.

Table 3. U-Pb ages already available for the region, obtained by means of different methods.

Number	Location	Rock type	Method	Age, MA	Reference
8697-8679	Minícia	Migmatite	TIMS	1859	Gaudette and Olszewski 1985
6580-6085	Casiquiare River	Tonalite	SHRIMP	1834 ± 18	Tassinari *et al.* 1996
8699	Macabana	Augen-gneiss	TIMS	1823	Gaudette and Olszewski 1985
MS-63	Iã-Mirim River	Monzogranite	SHRIMP	1810 ± 09	Santos *et al.* 2000
PR-3215	Araracuara	Syenogranite	ICP-MS	1756 ± 08	Ibañez-Mejia *et al.* 2011
J-263	Araracuara	Syenogranite	ICP-MS	1732 ± 17	Ibañez-Mejia *et al.* 2011
UA-39	Uaupés River	Qartz-diorite	TIMS	1703 ± 07	Tassinari *et al.* 1996
CRJ-19	Apaporis River	Syenogranite	ICP-MS	1593 ± 06	Ibañez-Mejia *et al.* 2011
PR-3092	Apaporis River	Syenogranite	ICP-MS	1578 ± 27	Ibañez-Mejia *et al.* 2011
UAH-1216	Vaupés River	Monzogranite	ICP-MS	1574 ± 10	Ibañez-Mejia *et al.* 2011
PRA-4	Mitu	Granite	TIMS	1552 ± 34	Priem *et al.* 1982
AH-1419	Apaporis River	Monzogranite	ICP-MS	1530 ± 21	Ibañez-Mejia *et al.* 2011
PA-22	Papuri River	Granite	SHRIMP	1521 ± 13	Tassinari *et al.* 1996
AF-151	Içana River	Two mica-granite	Pb evap.	1521 ± 32	Almeida *et al.* 1997
AF-1	São Gabriel	Granite with titanite	TIMS	1518 ± 25	Santos *et al.* 2000
PRA-21	Guainia River	Granite	TIMS	1480 ± 70	Priem *et al.* 1982

are euhedral and well preserved, presenting a prismatic habit. The length to width ratios range from 0.5:1 to 4:1, and lengths range from 0.12 to 0.37 μm. CL images reveal a complex to well-developed oscillatory zoning (e.g.. zircons 7.1 and 1.1 of Fig. 4B. The Concordia diagram (Fig. 5B) indicates a good-quality crystallization age of 1775.3 ± 7.7 Ma (MSWD = 1.2, n = 16) for the protolith.

PR-3141 – Biotite gneiss – Caño Cuaubén, near Puerto Inírida, Colombia

Sample PR-3141 is a fine-grained foliated biotite gneiss, very likely an orthogneiss, with a granolepidoblastic structure. Zircons of this rock are euhedral with a prismatic to sub-rounded habit. They range in length from 0.150 to 0.290 μm, with length to width ratios from 2:1 to 3:1. CL images reveal a complex to well-developed oscillatory zoning in most of the grains (e.g. zircons 6.1 and 9.1 in Fig. 4C). The Concordia diagram (Fig. 5C) shows a few discordant grains, but 15 grains near the Concordia, yield an age of 1501.0 ± 9.5 Ma (MSWD = 1.08, n = 15), which can be attributed to magmatic crystallization.

EP-2 – Biotite-gneiss – Caquetá River, near Araracuara, Colombia

Sample EP-2 is a probable biotite-muscovite orthogneiss, with a fine-grained granoblastic structure. Zircons of this sample are euhedral to subhedral, mostly with a prismatic habit. They range in size from 0.1 to 0.3 μm and have length to width ratios from 1:1 to 3:1. CL images reveal mostly oscillatory zoning (e.g. zircon 2.1 of Fig. 4D). Some points are discordant in the Concordia diagram (Fig. 5D), but a group of 10 grains located very close to the Concordia indicate an age of 1721.0 ± 9.6 Ma (MSWD = 1.8, n = 10) which is attributed to the crystallization of the igneous protolith.

J-84 – Monzogranite – Raudal Morroco, Inírida River, Colombia

Sample J-84 is a coarse-grained faneritic monzogranite with centimetric K-feldspar. Zircons of this rock are euhedral with a prismatic to sub-rounded habit. They range in length from 110 to 370 μm, with length to width ratios from 2:1 to 7:1. CL images reveal either sector or oscillatory zoning in most of the grains (e.g. zircons 2.1 and 3.1 of Fig. 4E). The Concordia diagram (Fig. 5E) indicates discordance of several grains. However, the age

calculation for 12 zircons near the upper intercept yield a reasonable crystallization age of 1507 ± 22 Ma (MSWD = 4.7, n = 13).

PR-3001 – Biotite-chlorite gneiss – Caño Cuduyarí, Vaupés River, near Mitú, Colombia

Sample PR-3001 is a coarse-grained biotite-chlorite gneiss, possibly an orthogneiss, with a granolepidoblastic structure. Zircons are euhedral to subhedral, and most have prismatic habit. They range in size from 110 to 400 µm and have length to width ratios from 1:1 to 3:1. CL images reveal mostly complex and well-developed oscillatory zoning (e.g. zircons 2.1 and 5.1 in Fig. 4F). In the Concordia diagram (Fig. 5F) zircons are mostly concordant. Age calculation of 12 selected zircon grains indicates a crystallization age of 1769 ± 33 Ma (MSWD = 1.9, n = 12).

J-199 – Biotite-hornblende orthogneiss – Negro river, north of San Carlos, Colombia/Venezuela

Sample J-199 is a biotite-hornblende orthogneiss rich in quartz, with a fine-grained lepidonematoblastic structure. Zircons from this rock range in size from 90 to 170 µm and have length to width ratios of less than 2:1. CL images reveal either sector or oscillatory zoning (e.g. zircons 6.1 and 3.1 in Fig. 4G). Zircons are mostly concordant. The age calculation for the Concordia diagram (Fig. 5G) indicates a quite precise crystallization age of 1796.1 ± 3.7 Ma (MSWD = 1.5, n = 12).

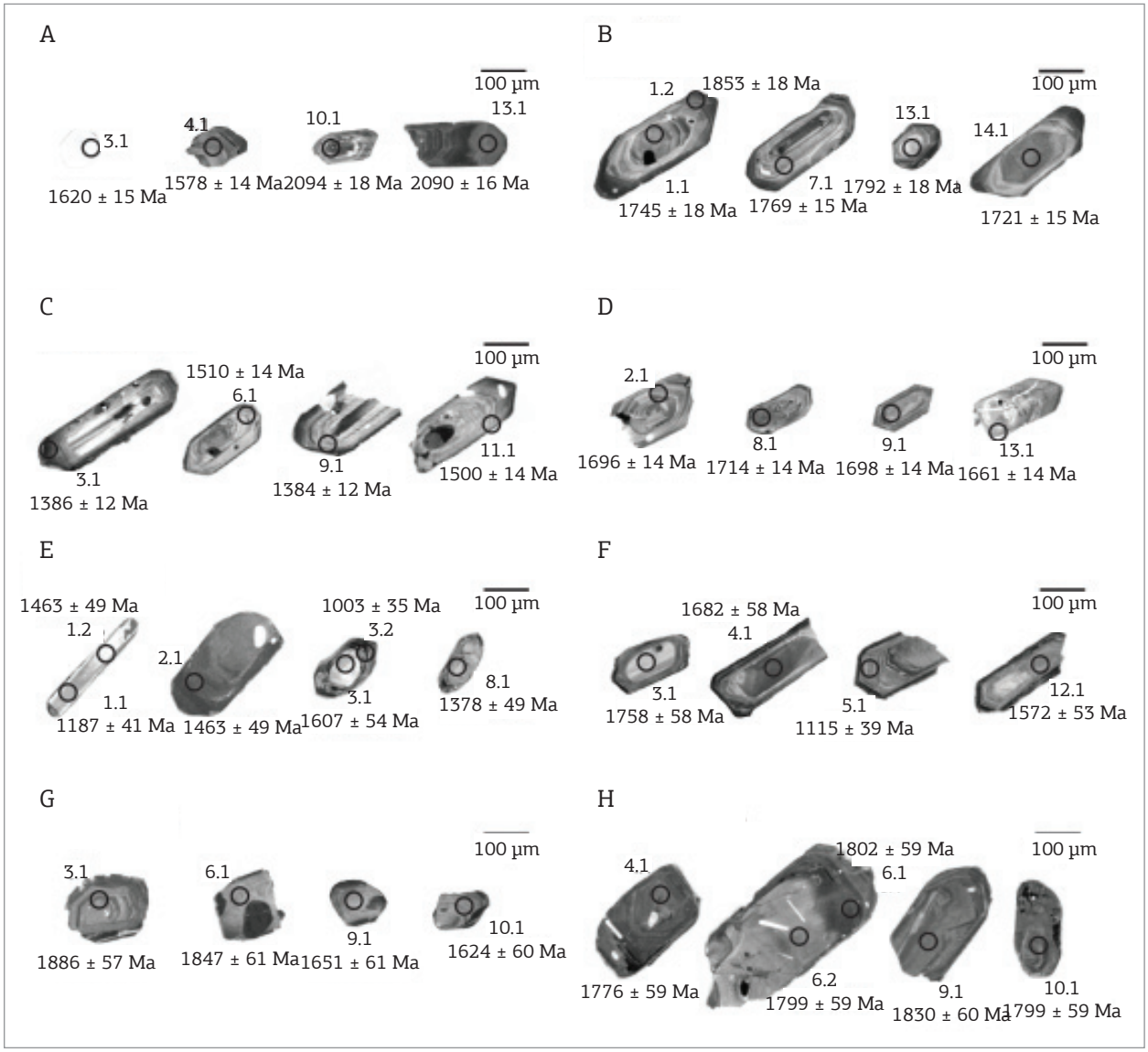

Figure 4. Example of zircons dated by the shrimp method. (A) Sample J-36; (B) Sample J-127; (C) Sample PR-3141; (D) Sample EP-2; (E) Sample J-84; (F) Sample PR-3001; (G) Sample J-199; (H) Sample HB-667.

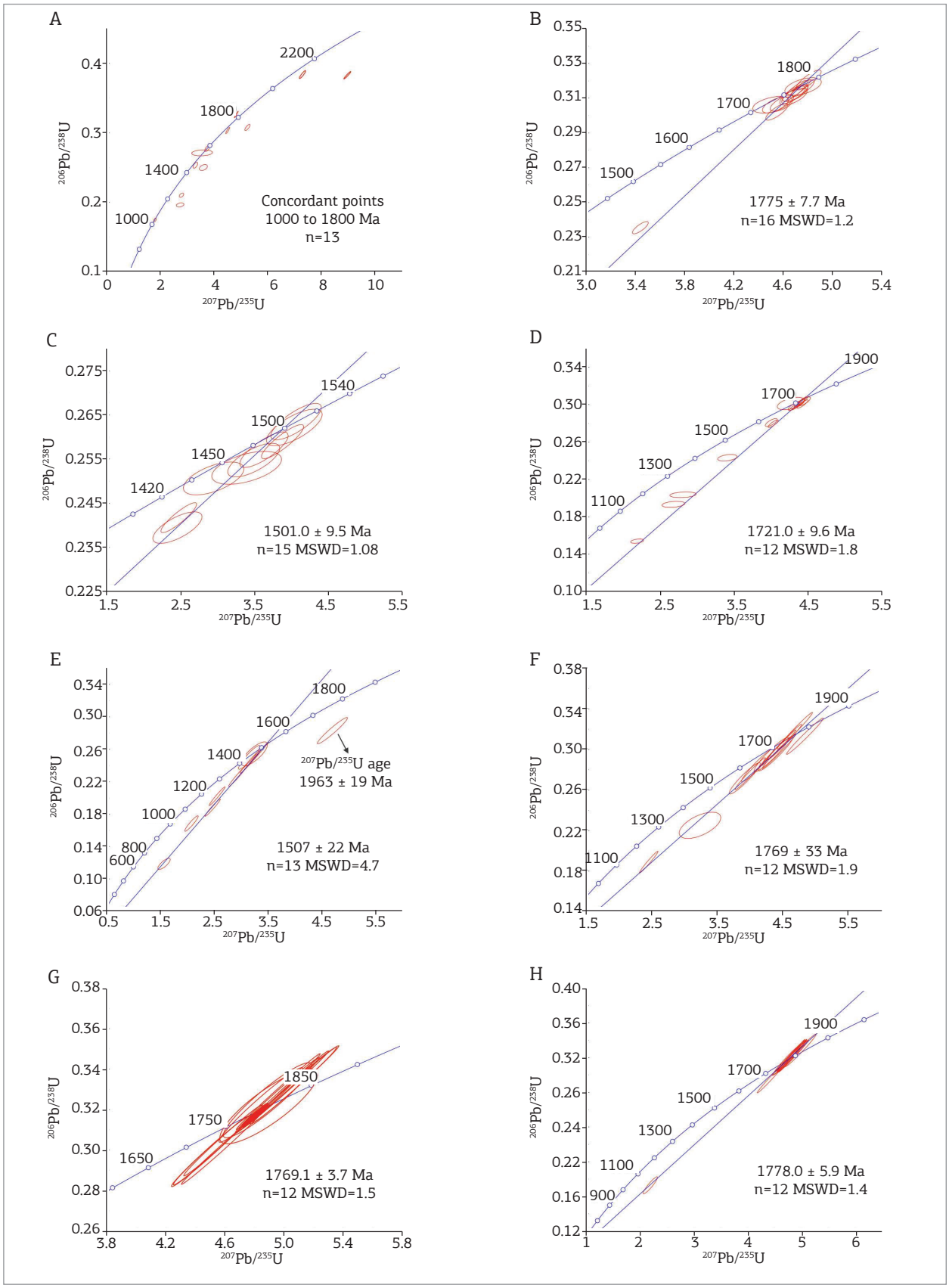

Figure 5. Concordia diagrams for the samples dated by shrimp. (A) J-36 Paragneiss; (B) J-127 Orthogneiss; (C) PR-3141M Orthogneiss; (D) EP-2 Orthogneiss; (E) J-84 Monzogranite; (F) J-84 Monzogranite; (G) J-199 Orthogneiss; (H) HB-667 Monzogranite.

HB-667 – Monzogranite – Raudal Carurú, Vaupés River, near Iauaretê, Brazil/Colombia

Sample HB-667 is a coarse grained faneritic monzogranite with biotite, hornblende and centimetric microcline phenocrysts. Zircons of this rock are subhedral with a sub-rounded habit. They range in length from 100 to 400 μm, with length to width ratios from 1:1 to 3:1. CL images reveal a complex oscillatory zoning in most of the grains (e.g. zircons 6.1 and 4.1 of Fig. 4H). Analyses of 12 concordant zircons (Fig. 5H) indicates a precise crystallization age of 1778.8 ± 5.9 Ma (MSWD = 1.4, n = 12).

The following U-Pb dates, obtained by WS, were reported in a preliminary form by Andrade-Santos (2010). Figure 2 shows the locations of the samples. Figs. 4A to 4G provides CL images of some selected zircons, and Figs. 5A to 5G the resulting Concordia diagrams.

AH-1213A – Biotite-hornblende orthogneiss – Raudal Tucunaré, Vaupés, SE of Mitú, Colombia

Sample AH-1213A is a biotite-hornblende orthogneiss characterized by a fine to medium grained granoblastic structure, with some lepidoblastic portions. Zircons from this rock range in size from 100 to 390 μm, with length to width ratios ranging from 1.5:1 to 4:1. The zircons are generally anhedral to subhedral and medium rounded. CL images reveal sector zoning (e.g. zircon 12, Fig. 6A). Analyses of 26 zircons yield a crystallization age for the protolith of 1736 ± 19 Ma (MSWD = 0.08, Fig. 7A).

AH-1231 – Monzogranite – Serrania Mitu, Colombia

Sample AH-1231 is a monzogranite with a medium to coarse-grained faneritic structure. Zircons are euhedral to subhedral, with a prismatic habit. They range in size from 200 to 400 μm and have length to width ratios from 1.5:1 to 2:1. CL images reveal mostly complex sector and oscillatory zoning (e.g. zircons 8 and 10 in Fig. 6B). Analyses of 23 selected zircons reveal concordance and a crystallization age of 1510 ± 26 Ma (MSWD = 0.15, Fig. 7B).

AH-1248 – Paragneiss – Caño Chaquita, Atabapo River, near Puerto Inírida

Sample AH-1248 is a paragneiss with a fine-grained structure and some muscovite. Zircons of this sample are euhedral, mostly with a prismatic habit. They range in size from 100 to 230 μm and have length to width ratios from 2:1 to 6:1. CL images reveal mostly oscillatory zoning (Fig. 6C). Analyses of 37 selected zircons reveal that most are discordant. Those close to the Concordia were plotted (Fig. 7C), with most being located between 1120 and 1550 Ma. One of the grains is located at about 650 Ma and its age and tectonic significance must be investigated further.

J-42 – Paragneiss – Mitú, Colombia

Sample J-42 is a paragneiss characterized by a medium to coarse-grained texture with some centimetric K-feldspar phenocrysts. Zircons of this rock are subhedral and medium rounded. They range in length from 120 to 260 μm, with length to width ratios from 1.5:1 to 2:1. CL images reveal sector and oscillatory zoning in most grains (e.g. zircons 13 and 9, Fig. 6D). Twenty-five detrital zircons were analyzed. Several grains are not far from the Concordia (Fig. 7D), located between 700 and 1900 Ma. Possible Neoproterozoic sources have not been identified in the area, and this metasedimentary unit must be investigated further.

J-98 – Monzogranite – Caño Nabuquén, Inírida River

Sample J-98 is a monzogranite comprised of medium- to coarse-grained faneritic rock. Zircons from this rock are mostly euhedral with a prismatic habit, sizes ranging from 100 to 320 μm, and length to width ratios from 1.6:1 to 3:1. CL images reveal oscillatory zoning in most grains with well preserved cores (e.g. zircon 2 in Fig. 6E). Twenty zircons were analysed, and a few of them are discordant. Fifteen grains close to the Concordia indicate a crystallization age of 1752 ± 21 MA (MSWD = 0.13, Fig. 7E)

J-159 – Tonalite – Serrania de Naquén, Guainia River, Colombia

Sample J-159 is a tonalite characterized by a medium to coarse-grained faneritic texture, with some muscovite. Zircons are mostly euhedral and well preserved, with a prismatic habit. Length to width ratios range from 1:1 to 3:1, and lengths range from 120 to 310 μm. CL images reveal a complex to well-developed oscillatory zoning (Fig. 6F). Analyses of 26 zircons revealed that most are concordant, with a crystallization age of 1770 ± 40 Ma (MSWD = 0.21, Fig. 7F).

PR-3228 – Paragneiss – Rio Mesai, Yarí, N of Araracuara, Colombia

Sample PR-3228 is a biotite gneiss, with microcline and some chlorite, characterized by a fine to medium granoblastic structure. Zircons of this rock are euhedral to subhedral with a prismatic habit. They range in length from 70 to 250 μm with length to width ratios from 1,3:1 to 4:1.

CL images reveal a complex oscillatory zoning in most of the grains (e.g. zircon 3, Fig. 6G) and some complex sector zoning. Thirty-eight zircons were analyzed and plotted in Fig. 7G. Although most of the zircons are discordant, nine grains are nearly concordant and yield detrital ages between 1800 and 1300 Ma. Older grains were not found.

SAMARIUM-NEODYMIUM MEASUREMENTS

Twenty-two Sm-Nd model ages are currently available for the study region (see Fig. 2 for sample locations and Tab. 2 for the analytical data). Twelve of these samples (described above) were also dated by the U-Pb zircon method.

Most samples yield very similar paleoproterozoic T_{DM} model ages (ca. 1.9 – 2.2 Ga, Tab. 2) although their U-Pb zircon ages varied within the 1800 – 1500 MA interval. Their calculated $\varepsilon_{Nd(TDM)}$ values were also similar (positive values of 3.0 – 3.5), suggesting formation from the same juvenile source material. Given that the $\varepsilon_{Nd(T1)}$ values of the granitoid rocks are near zero or slightly negative, the possible presence of much older source material is improbable. This finding reinforces the idea of accretion though subduction during the Proterozoic, as well as the presence of juvenile magmatic arcs in this part of the Rio Negro-Juruena province.

There is marked similarity in all trends in the Nd isotopic evolution diagram for the 11 granitoid rocks dated by the U-Pb zircon method (Fig. 8). Rocks with ages in the 1800 – 1750 Ma range exhibit $\varepsilon_{Nd(T1)}$ values close to zero, but 2 younger rocks (J-84 and PR-3141, ages around 1550 Ma) have moderately negative values. We suggest that these younger granitic rocks could have

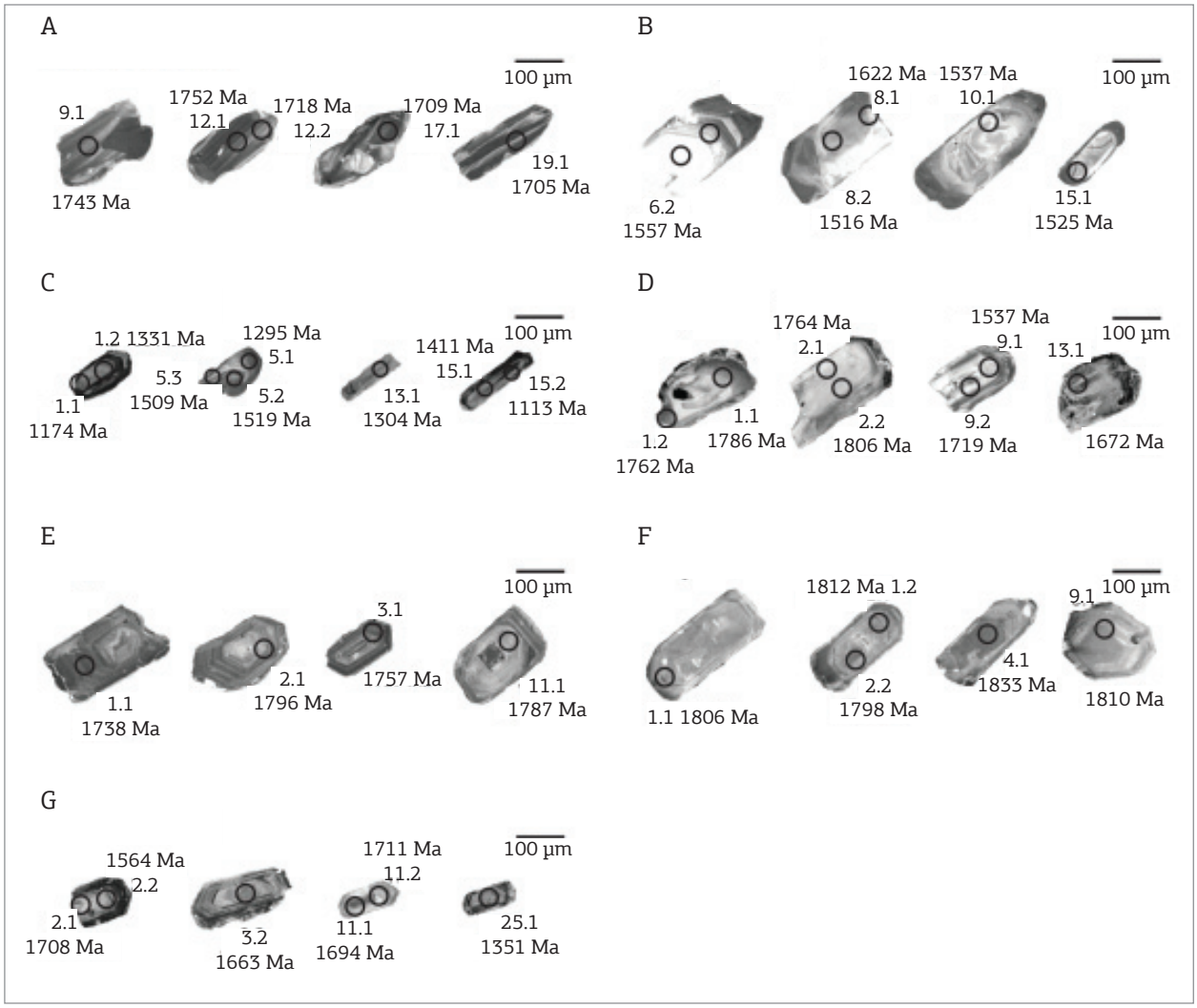

Figure 6. Example of zircons analysed by LA-ICP-MS method. (A) Sample AH-1213A; (B) Sample AH-1231; (C) Sample AH-1248; (D) Sample J-42; (E) Sample J-98; (F) Sample J-159; (G) Sample PR-3228.

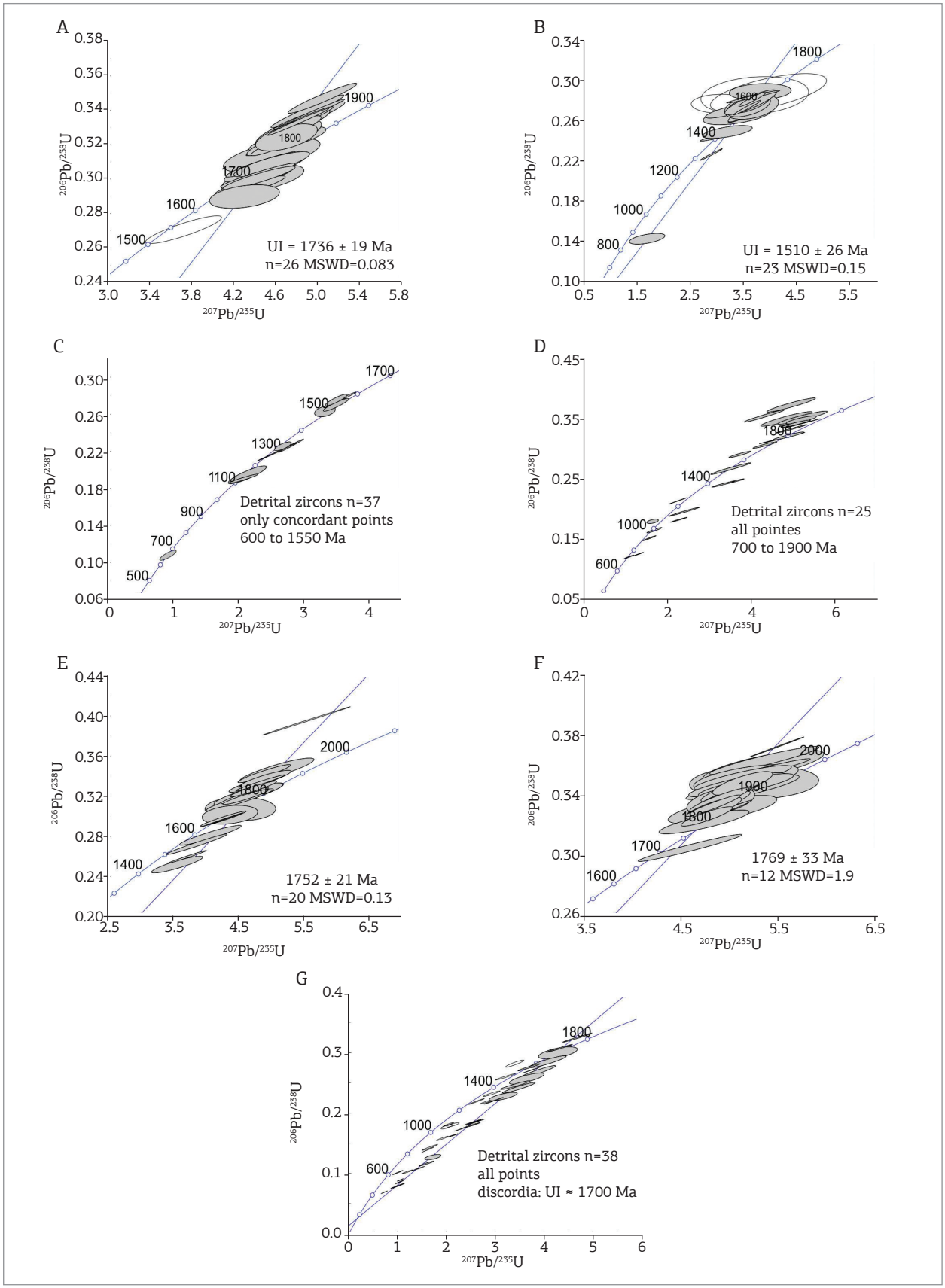

Figure 7. Concordia diagrams for the samples dated by LA-ICP-MS. (A) AH-1213A Orthogneiss; (B) AH-1231 Monzogranite; (C) AH-1248 Paragneiss; (D) J-42 Paragneiss; (E) J-98 Monzogranite; (F) PR-3001 Orthogneiss; (G) PR-3228 Paragneiss.

originated from the melting or complete reworking of the accretionary crustal material that formed about 200 to 250 Ma earlier.

INTERPRETATION OF THE RADIOMETRIC AGES

General remarks

A total of 97 granites, gneisses and migmatites within the studied region were analysed by the Rb-Sr method and selected for further interpretation (Fig. 3, Tab. 1). Some of the analyses were performed recently by the CPGeo-USP, but most of them were taken from the literature (Gaudette and Olszewski 1985, Priem *et al.*1982, Barrios *et al.*1985, Fernandes *et al.*1976, Pinheiro *et al.* 1976). An interpretative exercise was made to verify the possible temporal relationship among granitoid rocks located close enough to have been subjected to the same geological history. Potentially related samples were identified in eight areas (different colors in Fig. 3, Ventuari River, Atabapo River, Negro-Casiquiare Rivers, Puerto Inírida, San Carlos, Mitu-Iauaretê, Caquetá River and São Gabriel + Içana River).

Analytical points of the potentially related samples were included in isochron diagrams (Fig. 9A-H), each of which obtained in different works from different laboratories, with different equipment and precision levels. To "normalize" the calculations, we fixed the same values to the experimental errors of the calculated $^{87}Rb/^{86}Sr$ (3%) and $^{87}Sr/^{86}Sr$ (0.25%) results. This approach should minimize the preference for precise analytical results during the Isoplot calculations. As the granitoid samples in each diagram are not strictly cogenetic, the calculated isochron ages should be viewed as rough approximations for interpreting the overall tectonic history. Analytical points in all diagrams (Fig. 9) show reasonable alignments. As the calculated best-fit lines could be broadly interpreted as "isochron ages", with probable geological significance, they are referred as "reference isochrons". We speculate that these lines indicate, for each area, a regional event of Sr homogenization for the whole-rock system.

Atabapo belt

Gaudette and Olszewski (1985) collected seven samples of granitic-migmatitic rocks from the NE part of the study area along the Ventuari River between Minicia and Macabana

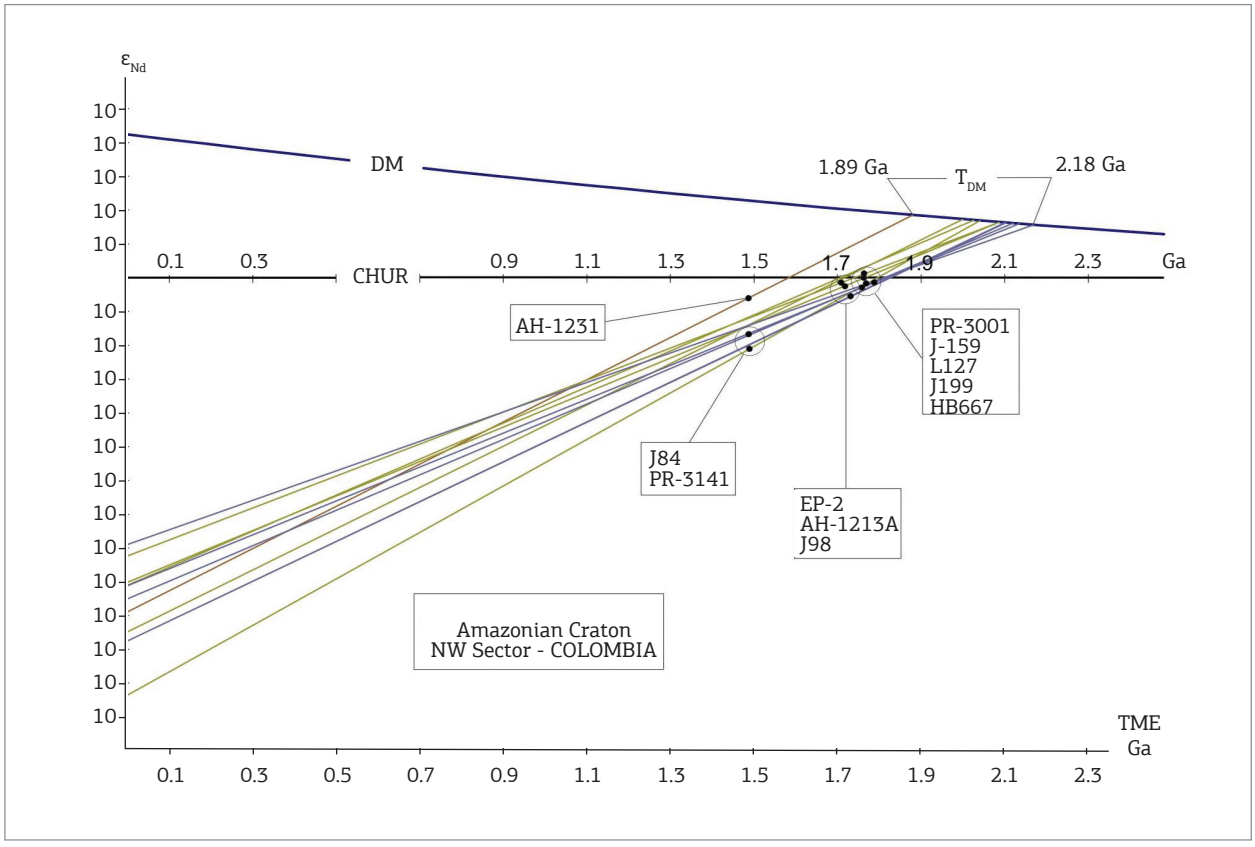

Figure 8. Nd evolution diagram.

(Venezuela). These rocks are located along a reference isochron of 1837 ± 87 Ma, with a low initial $^{87}Sr/^{86}Sr$ ratio of 0.7021 (Fig. 9A). Analysis of the same rocks by U-Pb zircon (TIMS) revealed concordant values of 1859 Ma at Minicia and 1823 Ma at Macabana (Tab. 3). Several authors (Gaudette and Olszewski 1985, Priem *et al.* 1982, Barrios *et al.*1985), collected 17 samples of granitoid rocks along the Atabapo River (Tab. 1). Their isochron diagram (Fig. 9B) indicated an apparent age of 1749 ± 92 Ma, with an initial $^{87}Sr/^{86}Sr$ ratio of 0.7073. A similar age span (1787 ± 53 Ma), with an initial $^{87}Sr/^{86}Sr$ ratio of 0.7025 (Fig. 9C), was obtained for samples from the Negro and Casiquiare Rivers, by Priem *et al.* (1982), Gaudette and Olszewski (1985), and the present work (Tab. 1).

Four isolated samples of granitoid rocks collected along the Inírida and Guainia Rivers yielded precise U-Pb zircon ages in the same range (Fig. 2, Tab. 3): J98(1772 ± 15 Ma), J-127 (1772 ± 4 Ma), J-159 (1785 ± 6 Ma) and J-199 (1796 ± 4 Ma). Considering the isolated U-Pb zircon ages and the Rb-Sr reference isochrones (Fig. 9B and 9C), we provisionally name this granitoid region of the Rio Negro-Juruena province as the "Atabapo belt". We propose that a series of orogenic pulses, lasting at least 60 Ma, from 1800 to 1740 Ma, in the late Paleoproterozoic (Statherian), was responsible for the development of this belt in the NE part of the study area.

We constructed another isochron diagram (Fig. 9D) from data of six samples of a non-deformed granite (Priem *et al.* 1982), and one sample of the present work (Tab. 1), obtained within the same corner near Puerto Inírida. The apparent age of these samples was 1476 ± 68 Ma, with an initial $^{87}Sr/^{86}Sr$ ratio of 0.7064. One sample of the present work (Tab. 1) and seven previously obtained granitic samples (Gaudette and Olszewski 1985, Priem *et al.* 1982, Barrios *et al.* 1985), all collected near the town of San Carlos at the Negro River, yielded an age of 1521 ± 52 Ma, with an initial $^{87}Sr/^{86}Sr$ ratio of 0.7051 (Fig. 9E). Three isolated granitic samples within the same region were dated by the U-Pb method (PR-3141: 1500 ± 9 Ma, J-84: 1507 ± 19 Ma, and PRA-2: 1480 ± 70 Ma; Tab. 3). The results confirm the intrusive age of some granitic intrusions into the Atabapo belt at about 1500 Ma, within the Mesoproterozoic (Calymmian).

Vaupés belt

Priem *et al.* (1982), Pinheiro *et al.* (1976) and Santos (2003) obtained and dated 27 samples of granitoid rocks from central area of the study region, between the villages of Mitú, Colombia, and Iauaretê, Brazil. A few samples from the same area were analysed by us (Tab. 1). A reference isochron (Fig. 9F) seems to indicate a mesoproterozoic (calymmian) Sr homogenization event at 1529 ± 43 Ma with an initial $^{87}Sr/^{86}Sr$ ratio of 0.7067. Within the same area, there are 8 U-Pb zircon ages (see Fig. 2 and Tab. 3). Four of them are clearly older, and have statherian apparent ages (AH-1213A: 1746 ± 8 Ma; PR-3001: 1740 ± 5 Ma; J-36: 1739 ± 38 Ma; HB-667: 1778 ± 4 Ma), whereas the 4 other are within the same age range as the Rb-Sr isochron (AH-1231: 1555 ± 7 Ma; AH-1216: 1574 ± 10 Ma; PA-SP-22: 1521 ± 13 Ma; PRA-4: 1552 ± 34 Ma). In this region, the younger granitoid rocks are described as calc-alkaline syntectonic gneisses and migmatites affected by medium-level amphibolite facies metamorphism (Priem *et al.* 1982, Santos 2003). Thus, we may conclude that the results of the Rb-Sr systematics indicate an episode of Sr isotopic homogenization of mesoproterozoic age related to that specific orogenic pulse.

We provisionally name this area "Vaupés belt". We postulate that the belt developed from a series of orogenic pulses in the Calymmian, with duration of at least 60 Ma, between 1580 and1520 Ma. Older statherian granitoid rocks in the region (U-Pb zircon age ~ 1750 Ma) may be considered as basement inliers. These rocks must have been involved within the younger calymmian metamorphism. A few younger and undeformed granitic rocks, whose points lie within the same reference isochron, could represent post-tectonic granitic batholiths.

Four samples by Priem *et al.* (1982) and one by us were obtained from the SW of the study area, near Araracuara. The reference isochron with these samples indicated an apparent age of 1557 ± 41 Ma, with an initial $^{87}Sr/^{86}Sr$ ratio of 0.7050 that was fixed in the age calculation (Fig. 9G). Older ages in the same area were obtained by Ibañez *et al.* (2011) from two syenogranitic gneisses (PR-3215: 1756 ± 8 Ma; J-263: 1732 ± 17 Ma) and sample EP-2 from this work 1725 ± 10 MA (Fig. 2 and Tab. 3). As was the case in the central Mitú-Iauaretê region, these older rocks could represent statherian basement rocks within younger mesoproterozoic metamorphic gneisses. However, for the same region, along the Apaporis river, the same authors encountered three other rocks with younger ages (CRJ-19: 1593 ± 6 Ma; PR-3092: 1578 ± 27 Ma; AH-1419: 1530± 21 Ma), reinforcing the idea of the existence of a Vaupés tectonic-metamorphic belt of calymmian age.

Regional thermal evolution

The initial Sr^{87}/Sr^{86} ratios encountered in the reference isochrones of Figs 9A to 9G (0.702 – 0.708), are considered relatively low and indicate an important participation of juvenile material. This possibility is supported by the Sm-Nd systematics. The only exception to the relatively low initial ratios was observed for samples from the Brazilian region along the Içana River and near the town of São Gabriel da

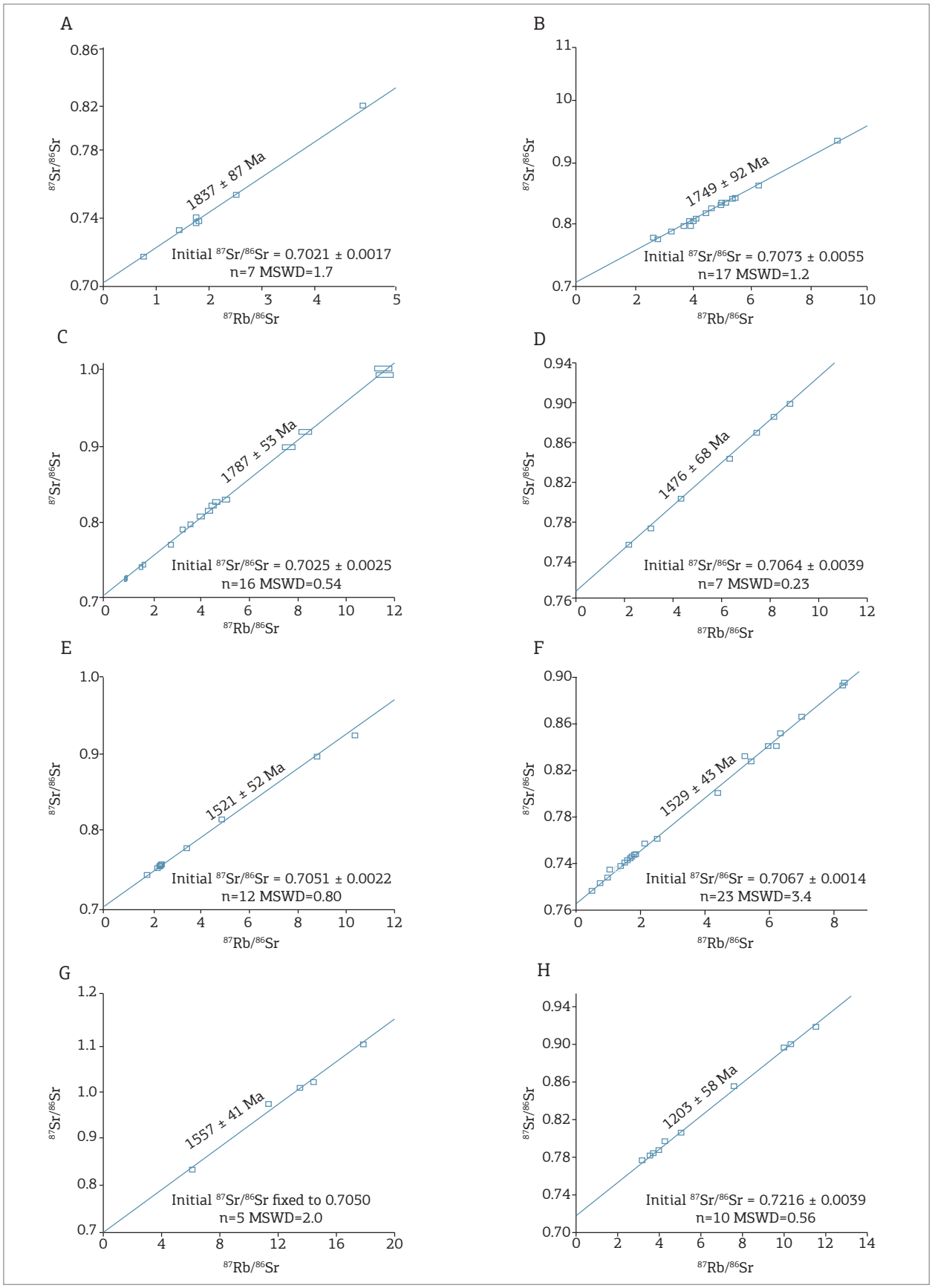

Figure 9. Rb-Sr whole-rock isochron diagrams. (A) Ventuari River; (B) Atabapo River; (C) Negro and Casiquiare rivers; (D) Puerto Inírida; (E) San Carlos; (F) Mitú-Iauaretê; (G) Caquetá River; (H) San Gabriel + Içana River.

Cachoeira (Fig. 9H). In this case, the reference isochron of 11 points yielded an apparent age of 1203 ± 58 Ma with a very high initial $^{87}Sr/^{86}Sr$ close to 0.72. This age, much younger than what was encountered for most domains within the study area, should be related to a very strong regional heating that imposed Sr isotopic redistribution in the whole-rock samples. This condition seems to have been localized to an elongated area separating the Atabapo and Vaupés belts (Fig.3), affected respectively by metamorphic belts with statherian and calymmian age.

About 100 K-Ar measurements, predominantly from micas, were made a few decades ago in rock samples from the study area. Complete analytical data of these measurements and sample locations can be found in Priem *et al.* (1982) for Colombia, Barrios *et al.* (1985) for Venezuela and Tassinari (1996) for Brazil. A histogram of all available apparent K-Ar ages (Fig.10) reveals that the ages are concentrated within the 1200 – 1400 Ma interval. This result reflects regional heating above 350 – 400ºC, which affected the entire territory of Figure 2 and beyond, covering much of the Amazonian Craton. This regional heating was first observed in the 1960's (Priem *et al.* 1971) and is called the Nickerie thermo-tectonic episode in Suriname and K'Mudku in the Guyana Republic (Gibbs, Barron 1993). Cordani *et al.* (2010) attempted a comprehensive review and tentative interpretation of this major intraplate heating episode, whose duration may have been of 100-to-200 Ma. It is clear that this mesoproterozoic thermal episode was pervasive and widespread in the Amazonian Craton.

TECTONIC HISTORY OF THE NW AMAZONIAN CRATON

General considerations

Robust geochronological tools are required when synthesizing the tectonic evolution of a very large region where basic geologic information is quite rare. Here, we employ four radiometric methods, each with its own interpretative value and tectonic significance. U-Pb measurements, either SHRIMP, ICP or TIMS, are essential for any geochronological work, because they produce significant punctual ages. However, alone, these measurements do not provide an entire geological history. They may indicate several magmatic events localized in time, but not their integration into a complete regional tectonic evolution. Rb-Sr whole-rock isochrones are less precise, but they indicate the timing of relevant episodes of Sr isotopic homogenization, related to medium- to high-grade metamorphic episodes. Sm-Nd model ages give insight into the type of the regional tectonic processes (e.g. intraplate or subduction-related, accretionary or collisional, juvenile or reworked). Finally, K-Ar ages, especially of micas, are related to the final cooling of the region, usually with respect to the principal episode of cratonization, or, alternatively, to some episodes of major intraplate crustal heating above 350 – 400ºC.

According to Cordani and Teixeira (2007), the Rio Negro-Juruena tectonic province of the Amazonian Craton (1.78 – 1.55 Ma) was formed by continued soft-collision/accretion processes driven by subduction, which produce a very large "basement" with the predominance of granitoid rocks, many of them with a juvenile-like Nd isotopic signature. Clear evidence of archean or paleoproterozoic basement has not yet been found in this region. This province is considered to be basically accretionary, formed from the complex juxtaposition of tectonic units, including intra-oceanic material, but also containing Cordilleran-type granites, collisional-type belts, volcanic-sedimentary basins, as well as post-tectonic and anorogenic-type complexes.

Summary of the tectonic history

Considering the geochronological pattern encountered in the Atabapo belt, we agree with Gaudette and Olszewski (1985), Barrios *et al.* (1985) and Cordani *et al.* (2000) that the possible NE boundary of the Rio Negro-Juruena province with the older Ventuari-Tapajós province would be located close to or along the Atabapo River (Fig. 2 and 3). The U-Pb zircon SHRIMP measurements indicate the formation of a series of statherian magmatic arcs in that region, in which juvenile and possibly intra-oceanic material predominates. Closely related to subduction, these magmatic arcs piled up by soft-collision episodes and successive stacking from SW to NE, encompassing a period of about 60 Ma.

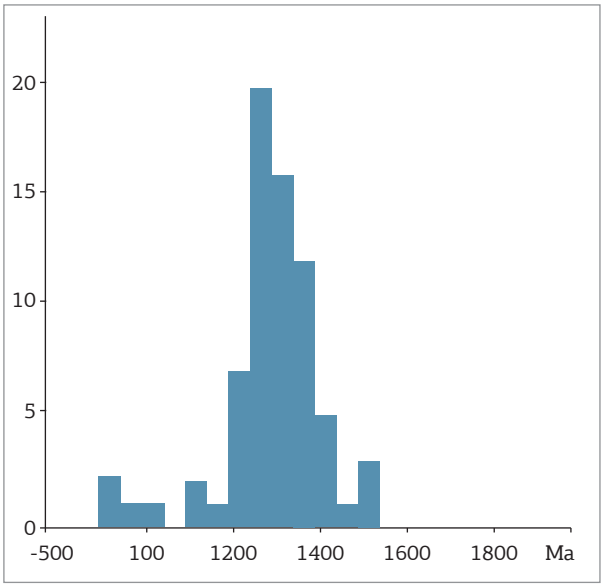

Figure 10. Histogram of K-Ar ages on micas.

In the SW region, comprising the Mitú-Iauaretê and Caquetá River areas, calymmian granitic and gneissic rocks formed between 1580 and 1500 Ma within the Vaupés belt. These calymmian ages can be confirmed by the U-Pb zircon ICP-MS ages obtained by Ibañez *et al.* (2011) on granitic rocks collected along the Apoporis River (see Fig. 2), well inside the younger belt. Results of the Sm-Nd systematics for rocks of the Vaupés belt indicate the presence of substantial juvenile material. An important time-gap of 150-to-200 Ma exists between the youngest rocks of the Atabapo belt (1740 Ma) and the oldest rocks of the Vaupés belt (1580 Ma). The latter are products of a second orogenic pulse within the same Rio Negro-Juruena tectonic province. Thus, there is ample time for cratonization of the first series of tectonic belts before the stacking of the second series of possibly accretionary belts in Mesoproterozoic time. At the NE corner, a cratonized 1740 – 1800 Ma basement was intruded by granitic batholiths at 1550 Ma, which may correspond to the reflection of the orogenic pulse occurring at that time to the SW. However, at the SW corner, the second 1580 – 1500 Ma orogenic pulse includes parts of possibly retrogressed basement inliers with ages of about 1750 Ma.

Gorayeb *et al.* (2005) showed that the NW part of the Rio Negro-Juruena province continues to the SE below the Solimões sedimentary basin, where its basement presents a few U-Pb zircon evaporation ages in the 1800 – 1550 Ma range. Geochronological control in the SE half of the province, in Mato Grosso, Brazil, shows that the ages of the granitoid rocks decrease from NNE to SSW. Near the boundary with the older Ventuari-Tapajós province, in the region of Alta Floresta, Santos (2003) encountered ages of 1780 Ma in the São Romão and São Pedro granites. On the other side, near the border with the Rondonian-San Ignacio belt, in the Alto Jauru region of Mato Grosso, Geraldes *et al.* (2001) reported the age of the Cachoeirinha magmatic arc as 1590 Ma. We found a comparable age pattern for the NW part of the Amazonian Craton (Fig. 3), where calc-alkaline orogenic type rocks yielded ages of 1800-to-500 Ma, decreasing from the NE (Atabapo belt) to the SW (Vaupés belt).

Thermal history

Finally, a peculiar but remarkable aspect of the tectonic evolution of this area is the widespread Nickerie-K'Mudku intraplate mid-proterozoic regional heating. This phenomenon affected all the rock units of the study area, from about 1400-to-1200 Ma (see histogram of Fig. 10). This regional heating episode, with temperatures exceeding 300°C, was uniform and affected the entire crust of the study area. The episode affected very large parts of the Amazonian Craton, and its duration may have been on the order of 100 – 200 Ma. All the rock ages determined by U-Pb zircon measurements are much older (1800 – 1500 Ma). Regardless of their ages, all rocks were affected in the same way. Therefore, none of the K-Ar apparent ages likely represents a primary magmatic age of the corresponding dated rock. Considering the Rb-Sr systematics of the region, the Rb-Sr reference isochron age (1200 ± 60 Ma) and the high initial $^{87}Sr/^{86}Sr$ ratio (~ near 0.720; Fig. 3 and 9G), we can make some additional speculations from the K-Ar ages. Rocks in the area of São Gabriel da Cachoeira and the Içana River, in NW Brazil, are well within the Rio Negro-Juruena province, and very likely have primary ages between 1800 and 1500 MA, as suggested by the U-Pb zircon ages. However, the rocks were perhaps heated to as high as 600°C, which would be necessary to produce the observed widespread Sr isotopic homogenization in the whole-rock systems. This very high heating event seems to have been restricted to the territory located more or less between the Atabapo and Vaupés belts (see Fig. 3).

CONCLUSIONS

From the currently available data, we suggest the following possible tectonic-thermal history for the overall region:

1. Formation of the first orogenic pulse of the province, the Atabapo belt, with stacking of magmatic arcs of the Atabapo-Negro-Casiquiare region against the cratonic area formed by the Ventuari-Tapajós continent, at 1800 – 1740 Ma.
2. Formation of the second orogenic pulse related to the Vaupés belt, with stacking of the Mitú-Iauretê and Caquetá magmatic arcs against the already cratonized area of the first pulse, at 1580 – 1500 Ma.
3. Onset of the Nickerie-K'Mudku intraplate regional heating to above 300°C within the entire region at 1200 – 1300 Ma, but attaining 600°C in the belt separating the first (Atabapo) and second (Vaupés) orogenic pulses.
4. The probable existence of younger metasedimentary units such as the paragneisses J-36, J-42, AH-1248 and PR-3228, which contain young detrital zircons of meso and neoproterozoic age, should be investigated.

ACKNOWLEDGEMENTS

We acknowledge help received from the staff of the Geochronology Research Center (CPGeo -USP), especially Ivone Sonoki for geochronological calculations and Vasco

Loios for zircon s eparation. We thank geologist Guilherme Andrade Santos for his aid during the preliminary phase of the work. W.R. Van Schmus and M. Ibañez-Mejia are acknowledged for their much appreciated and important revision of the original version of our manuscript. INGEOMINAS of Colombia provided the samples and valuable geological information for this research. Financial support was received from FAPESP through grant 2013/12754-0 to UGC.

REFERENCES

Almeida M.E., Fraga L.M.B., Macambira M.J.B. 1997. New geochronological data of calc-alkaline granitoids of Roraima State. *In*: South American Symposium on Isotope Geology, Campos do Jordão, *Extended Abstracts*, 34-35.

Almeida M.E. 2006. *Evolução geológica da porção centro-sul do Escudo das Guianas com base no estudo geoquímico, geocronológico e isotópico dos granitóides Paleoproterozóicos do sudeste de Roraima, Brasil.* Doctoral Thesis, CPGG-UFPA, 227 p. Unpublished.

Andrade-Santos G. 2010. *Determinações geocronológicas pelo método U-Pb em zircões do Craton Amazônico colombiano.* Monografia de Trabalho de Formatura, Instituto de Geociências, USP, São Paulo, 52 p. Unpublished.

Barrios F.J. 1983. *A caracterização geocronológica da região amazônica da Venezuela.* MS Dissertation, Instituto de Geociências, USP, 123 p.

Barrios F., Rivas D., Cordani U., Kawashita K. 1985. Geocronologia del Territorio Federal Amazonas. Memoria I Simposium Amazónico, Puerto Ayacucho, Venezuela, *Boletín de Geología*, Publicación Especial 10, pp. 22–31.

Barrios F., Cordani U.G., Kawashita K. 1986. Caracterización geocronologica del Territorio Federal Amazonas, Venezuela. *In*: VI Congreso Geologico Venezolano, *Actas*, v. 3, p. 1432-1480.

Cordani U.G., Tassinari C.C.G., Teixeira W., Kawashita K., Basei M.A.S. 1979. Evolução Tectônica da Amazônia com base nos dados geocronológicos. *Actas II Congreso Geologico Chileno*, pp. J-137-148.

Cordani U.G., Sato K., Teixeira W., Tassinari C.C.G., Basei M.A.S. 2000. Crustal evolution of the South American platform. *In*: Cordani U.G., Milani E.J., Thomas-Filho A., Campos D.A. (eds.). *Tectonic evolution of South America.* 31st International Geological Congress, Rio de Janeiro, p. 19-40.

Cordani U.G., Teixeira W. 2007. Proterozoic accretionary belts in the Amazonian Craton. *In*: Hatcher R.D. Jr., Carlson M.P., McBride J.H., Martinez-Catalan J.R. (eds.). *4-D Framework of Continentel Crust*. Geological Society of America, Boulder, Colo, USA, Memoir 200:297-320.

Cordani U.G., Fraga L.M., Reis N., Tassinari C.C.G., Brito-Neves B.B. 2010. On the origin and tectonic significance of the intra-plate events of Grenvillian-type age in South America: A discussion. *Journal of South American Earth Sciences*, **29**:143-149.

Fernandes P.E.C.A., Pinheiro S.S., Montalvão R.M.G., Issler R.S., Abreu A.S., Tassinari C.C.G. 1976. Cap. I – Geologia. *In*: DNPM, Brasil – Projeto RADAMBRASIL, Folha SA19 – *Içá*, p. 17-123.

Gaudette H.E., Olszewski Jr. W.J. 1985. Geochronology of the basement rocks, Amazonas Territory, Venezuela and the tectonic evolution of the western Guyana Shield. *Geologie en Mijnbouw*, **64**:131-143.

Geraldes M.C., Van Schmus W.R., Condie K.C., Bell S., Teixeira W., Babinski M., 2001. Proterozoic geologic evolution of the SW part of the Amazonian craton in Mato Grosso state, Brazil. *Precambrian Research*, **111**:91-128.

Gibbs A.K., Barron C.N. 1993. *The Geology of the Guiana Shield*. Oxford University Press, Claredon Press, New York, Oxford, 245 p.

Gorayeb P.S.S., Moura C.A.V., Barbosa R.C.O., Matsuda N.S. 2005. Caracterização do embasamento da Bacia do Solimões com base em dados petrográficos e geocronológicos em testemunhos de sondagem. *Contribuições à Geologia da Amazônia*, **4**:7-15.

Ibañez-Mejia M., Ruiz J., Valencia VA., Cardona A., Gehrels G.E., Mora A.R. 2011. The Putumayo Orogen of Amazonia and its implications for Rodinia reconstructions: New U-Pb geochronological insights into the Proterozoic tectonic evolution of northwestern South America. *Precambrian Research*, **191**:58-77.

Ludwig K.R. 2009. SQUID 2: A User's Manual, rev. 12 April 2009. *Berkeley Geochronological Center*, Special Publication 5, 110 p.

Pinheiro S.S., Fernandes P.E.C.A., Pereira E.R., Vasconcelos P.G., Pinto A.C., Montalvão R.M.G., Issler R.S., Dall'Agnol R., Teixeira W., Fernandes C.A.C. 1976. Cap. I – Geologia. *In*: DNPM, Brasil – Projeto RADAMBRASIL, Folha NA19, *Pico da Neblina*, p. 19-137.

Pinson W.H., Hurley P.M., Mencher E., Fairbairn H.W. 1962. K–Ar and Rb–Sr ages of biotites from Colombia, South America. *Geological Society of America Bulletin*, **73**:807-810.

Priem H.N.A., Boelrijk N.A.I.M., Hebeda E.H., Verdumen E.A.Th., Verschure R.H. 1971. Isotopic ages of the Trans-Amazonian acidic magmatism and the Nickerie metamorphic episode in the Precambrian basement of Suriname, South America. *Geological Society of America Bulletin*, **82**:1667-1680.

Priem H.N.A., Andriessen P.A.M., Boelrijk N.A.I.M., De Boorder H., Hebeda E.H., Huguett A., Verdurmen E.A.Th., Verschure R.H. 1982. Geochronology of the Precambrian in the Amazonas region of southeastern Colombia (western Guiana Shield). *Geologie en Mijnbow*, **61**:229-242.

PRORADAM. 1979. *La Amazonia Colombiana y sus recursos*. Proyecto Radargramétrico del Amazonas, Bogotá, 590 p.

Santos J.O.S., Hartman L.A., Gaudette H.E., Groves D.I., McNaughton N.J., Fletcher I.R. 2000. A new understanding of the Provinces of the Amazon Craton Based on Integration of Field Mapping and U-Pb and Sm-Nd Geochronology. *Gondwana Research*, **3**(4):453-488.

Santos J.O.S. 2003. Geotectônica dos Escudos das Guianas e Brasil Central. *In*: Bizzi L.A., Schobbenhaus C, Vidotti R.M., Gonçalves J.H. (eds.). *Geologia, Tectônica e Recursos Minerais do Brasil:* texto, mapas e SIG – CPRM – Serviço Geológico do Brasil, **4**:169-226.

Sato K., Tassinari C.C.G. 1997. Principais eventos de acreção continental no Craton Amazônico baseados em idades modelo Sm-Nd, calculada em evoluções estagio único e estagio duplo. *Contribuições à Geologia da Amazônia*, **2**:91-142.

Sato K., Tassinari C.C.G., Kawashita K. Petronilho L. 1995. O método gecronológico Sm-Nd no Igc-USP e suas aplicações. *Anais da Academia Brasileira de Ciências*, **67**(3):313-336.

Sato K., Tassinari C.C.G., Basei M.A.S., Siga Jr. O., Onoe A.T., Souza M.D. 2014. Sensitive High Resolution Ion Microprobe (SHRIMP IIe/MC) of the Institute of Geosciences of the University of São Paulo, Brazil: analytical method and first results. *Geologia USP*, Série Científica, **14**(3):3-14.

Stacey J.S., Kramers J.D. 1975. Approximation of terrestrial lead isotope evolution by a two-stage model. *Earth and Planetary Science Letters*, **26**(2):207-221.

Tassinari C.C.G. 1996. *O mapa geocronológico do Craton Amazônico no Brasil: revisão dos dados isotópicos.* Concurso de Livre Docência do Instituto de Geociências da USP, São Paulo.

Tassinari C.C.G., Macambira M.J.B. 1999. Geochronological provinces of the Amazonian Craton. *Episodes*, **22**(3):174-182.

Tassinari C.C.G., Cordani U.G., Nutman A.P., Van Schmus W.R., Bettencourt J.S., Taylor P.N. 1996. Geochronological systematics on basement rocks from the Juruena – Rio Negro Province (Amazonian Craton) and tectonic implications. *International Geology Review*, **38**:161-175.

Teixeira W., Tassinari C.C.G., Cordani U.G., Kawashita K. 1989. A review of the geochronology of the Amazonian Craton: tectonic implications. *Precambrian Research*, **42**:213-227.

Williams I.S. 1998. U-Th-Pb geochronology by ion microprobe. *In*: McKibben M.A., Shanks I., Ridley W.C.P., Ridley W.I. (eds.). *Applications of Microanalytical Techniques to Understanding Mineralizing Process* (1-35). Reviews in Economic Geology, Socorro, USA.

Available at www.sbgeo.org.br

Annex I. Isotope ratio data for samples analysed by LA-ICP-MS method.

Sample	Spot	Ratios											Ages				206/238
		207/235	1σ err	206/238	1σ err	coef. corr	238/206	1σ err	207/206	1σ err	208/206	1σ err	T206/238	1σ err	T207/206	1σ err	207/206
AH1213A	9.1	4.3892	0.1505	0.2985	0.0031	0.940	3.3504	0.0342	0.1067	0.0034	0.2088	0.0043	1.684	0.015	1.743	0.059	96
AH1213A	11.1	4.4771	0.1615	0.3002	0.0033	0.600	3.3316	0.0367	0.1082	0.0039	0.1005	0.0273	1.692	0.016	1.769	0.065	95
AH1213A	12.1	4.4426	0.1415	0.3007	0.0028	0.920	3.3257	0.0312	0.1072	0.0031	0.1707	0.0728	1.695	0.014	1.752	0.054	96
AH1213A	3.1	4.4305	0.1466	0.3022	0.0029	0.960	3.3091	0.0323	0.1063	0.0033	0.0642	0.0024	1.702	0.015	1.737	0.056	97
AH1213A	4.1	4.4941	0.1577	0.3061	0.0032	0.840	3.2669	0.0343	0.1065	0.0036	0.1860	0.0089	1.721	0.016	1.740	0.062	98
AH1213A	13.1	4.5635	0.1892	0.3139	0.0040	0.660	3.1862	0.0407	0.1055	0.0044	0.1462	0.0255	1.760	0.020	1.722	0.076	102
AH1213A	8.1	4.3386	0.1450	0.2947	0.0029	0.920	3.3936	0.0332	0.1068	0.0032	0.2295	0.0115	1.665	0.014	1.745	0.055	95
AH1213A	7.1	4.5632	0.1486	0.3087	0.0030	0.830	3.2399	0.0312	0.1072	0.0033	0.1839	0.0278	1.734	0.015	1.753	0.056	98
AH1213A	5.1	4.4900	0.1499	0.3088	0.0031	0.940	3.2387	0.0321	0.1055	0.0034	0.1804	0.0474	1.735	0.015	1.722	0.060	100
AH1213A	1.1	4.6893	0.1520	0.3212	0.0031	0.970	3.1133	0.0297	0.1059	0.0033	0.0560	0.0033	1.796	0.015	1.730	0.057	103
AH1213A	16.1	4.6858	0.1311	0.3223	0.0035	0.940	3.1023	0.0340	0.1054	0.0028	0.1857	0.0110	1.801	0.017	1.722	0.049	104
AH1213A	17.1	4.6575	0.1364	0.3227	0.0037	0.900	3.0988	0.0355	0.1047	0.0030	0.1521	0.0417	1.803	0.018	1.709	0.052	105
AH1213A	10.1	4.7158	0.1506	0.3231	0.0030	0.780	3.0951	0.0289	0.1059	0.0031	0.2427	0.0151	1.805	0.015	1.729	0.055	104
AH1213A	12.2	4.7058	0.1211	0.3243	0.0032	0.570	3.0831	0.0303	0.1052	0.0026	0.2174	0.0201	1.811	0.016	1.718	0.045	105
AH1213A	20.2	4.7240	0.1296	0.3262	0.0035	0.660	3.0652	0.0325	0.1050	0.0027	0.2032	0.0035	1.820	0.017	1.715	0.048	106
AH1213A	19.1	4.7352	0.1239	0.3288	0.0033	0.880	3.0413	0.0303	0.1044	0.0026	0.0795	0.0070	1.833	0.016	1.705	0.045	107
AH1213A	21.1	4.7694	0.1408	0.3299	0.0039	0.940	3.0312	0.0357	0.1049	0.0030	0.0616	0.0657	1.838	0.019	1.712	0.053	107
AH1213A	20.1	4.7958	0.1337	0.3317	0.0036	0.890	3.0152	0.0327	0.1049	0.0028	0.1516	0.0099	1.846	0.017	1.712	0.050	107
AH1213A	10.2	4.8165	0.1201	0.3333	0.0032	0.990	2.9999	0.0284	0.1048	0.0025	0.2440	0.0453	1.855	0.015	1.711	0.044	108
AH1213A	18.1	4.8432	0.1266	0.3338	0.0034	0.970	2.9956	0.0301	0.1052	0.0026	0.2042	0.0045	1.857	0.016	1.718	0.046	108
AH1213A	13.2	4.9062	0.1458	0.3352	0.0040	0.960	2.9832	0.0352	0.1061	0.0031	0.1291	0.0184	1.864	0.019	1.734	0.054	107
AH1213A	14.1	4.9491	0.1284	0.3384	0.0034	0.990	2.9555	0.0298	0.1061	0.0027	0.2513	0.0346	1.879	0.017	1.733	0.047	108
AH1213A	11.2	4.9057	0.1432	0.3395	0.0039	0.970	2.9459	0.0341	0.1048	0.0031	0.1282	0.0151	1.884	0.019	1.711	0.054	110
AH1213A	15.1	5.0493	0.1352	0.3471	0.0036	0.960	2.8808	0.0302	0.1055	0.0027	0.1168	0.0255	1.921	0.017	1.723	0.048	111
AH1213A	6.1	4.3024	0.1376	0.2898	0.0028	0.370	3.4501	0.0336	0.1077	0.0033	0.2560	0.0032	1.641	0.014	1.760	0.057	93
AH1213A	2.1	3.7228	0.1492	0.2706	0.0033	0.880	3.6957	0.0445	0.0998	0.0040	0.0758	0.0247	1.544	0.016	1.620	0.072	95
AH 1231	13.1	3.4623	0.1005	0.2669	0.0029	0.860	3.7461	0.0402	0.0941	0.0025	0.2184	0.0887	1.525	0.015	1.510	0.051	101
AH 1231	4.3	3.4966	0.1142	0.2669	0.0031	0.890	3.7472	0.0438	0.0950	0.0030	0.3226	0.0533	1.525	0.016	1.529	0.060	99
AH1231	7.1	3.3965	0.2637	0.2667	0.0040	0.530	3.7499	0.0569	0.0924	0.0075	0.5288	0.0169	1.524	0.021	1.475	0.151	103
AH1231	1.1B	3.2974	0.2081	0.2718	0.0033	0.840	3.6786	0.0443	0.0880	0.0059	0.2046	0.0224	1.550	0.017	1.382	0.130	112
AH 1231	15.1	3.5769	0.1154	0.2735	0.0032	0.780	3.6567	0.0430	0.0949	0.0028	0.3062	0.0531	1.558	0.016	1.525	0.056	102
AH 1231	8.2	3.5681	0.1054	0.2741	0.0030	0.930	3.6484	0.0400	0.0944	0.0026	0.1442	0.0685	1.562	0.015	1.516	0.051	102
AH 1231	9.1	3.5838	0.1083	0.2744	0.0030	0.800	3.6439	0.0404	0.0947	0.0027	0.2152	0.0839	1.563	0.015	1.522	0.054	102
AH 1231	6.2	3.6575	0.2077	0.2750	0.0051	0.370	3.6364	0.0678	0.0965	0.0058	0.3662	0.0210	1.566	0.026	1.557	0.113	100
AH 1231	12.1	3.6004	0.1679	0.2755	0.0043	0.520	3.6303	0.0565	0.0948	0.0046	0.3525	0.0120	1.568	0.022	1.524	0.091	102
AH 1231	7.2	3.6374	0.1325	0.2770	0.0035	0.960	3.6099	0.0461	0.0952	0.0033	0.3690	0.0171	1.576	0.018	1.533	0.065	102

Continue...

Annex I. Continuation.

Sample	Spot	Ratios											Ages				206/238
		207/235	1σ err	206/238	1σ err	coef. corr	238/206	1σ err	207/206	1σ err	208/206	1σ err	T206/238	1σ err	T207/206	1σ err	207/206
AH 1231	10.1	3.6636	0.1434	0.2783	0.0038	0.730	3.5926	0.0489	0.0955	0.0037	0.4439	0.0353	1.583	0.019	1.537	0.071	102
AH 1231	1.3	3.6444	0.1996	0.2795	0.0051	0.860	3.5777	0.0657	0.0946	0.0056	0.5027	0.0624	1.589	0.026	1.519	0.115	104
AH1231	2.1	3.6879	0.2044	0.2851	0.0026	0.980	3.5077	0.0319	0.0938	0.0052	0.2085	0.0050	1.617	0.013	1.505	0.104	107
AH 1231	11.1	3.6759	0.1043	0.2826	0.0030	0.950	3.5392	0.0377	0.0944	0.0025	0.1908	0.0655	1.604	0.015	1.515	0.049	105
AH 1231	14.1	3.5750	0.1042	0.2742	0.0030	0.980	3.6469	0.0393	0.0946	0.0025	0.1895	0.0676	1.562	0.015	1.519	0.051	102
AH1231	3.1	3.8222	0.2374	0.2901	0.0033	0.160	3.4473	0.0398	0.0956	0.0060	0.1232	0.0386	1.642	0.017	1.539	0.124	106
AH1231	2.2	1.6920	0.1370	0.1430	0.0022	0.550	6.9950	0.1063	0.0858	0.0070	0.4270	0.0723	0.861	0.012	1.335	0.156	64
AH1231	4.2	3.1451	0.1859	0.2465	0.0024	0.960	4.0574	0.0400	0.0926	0.0053	0.1447	0.0381	1.420	0.012	1.479	0.109	96
AH1231	4.1	3.2009	0.1919	0.2498	0.0026	0.610	4.0029	0.0422	0.0929	0.0057	0.1463	0.0098	1.438	0.014	1.486	0.117	96
AH 1231	16.1	2.8970	0.0846	0.2272	0.0024	0.990	4.4022	0.0472	0.0925	0.0025	0.2449	0.0105	1.320	0.013	1.478	0.051	89
AH1231	1.2N	3.7190	0.4141	0.2860	0.0077	0.190	3.4966	0.0937	0.0943	0.0127	0.3542	0.0479	1.621	0.039	1.514	0.260	107
AH1231	8.1	3.9770	0.4464	0.2887	0.0078	0.640	3.4637	0.0933	0.0999	0.0124	0.4023	0.0413	1.635	0.039	1.622	0.246	100
AH1231	6.1	3.0984	0.2348	0.2777	0.0039	0.010	3.6011	0.0505	0.0809	0.0064	0.3837	0.0319	1.580	0.020	1.220	0.157	129
AH 1248	27.1	2.6027	0.1252	0.2195	0.0040	0.999	4.5552	0.0840	0.0860	0.0045	0.0993	0.0323	1.279	0.022	1.338	0.104	95
AH 1248	15.1	2.7574	0.0560	0.2239	0.0021	0.990	4.4655	0.0412	0.0893	0.0020	0.2537	0.0357	1.303	0.011	1.411	0.044	92
AH 1248	8.2	2.6882	0.0529	0.2255	0.0020	0.760	4.4340	0.0401	0.0864	0.0018	0.1131	0.0105	1.311	0.011	1.348	0.041	97
AH 1248	16.1	2.8489	0.0646	0.2276	0.0024	0.990	4.3940	0.0454	0.0908	0.0019	0.1050	0.0240	1.322	0.012	1.442	0.040	91
AH 1248	5.3	3.5078	0.0801	0.2705	0.0028	0.920	3.6973	0.0388	0.0941	0.0023	0.3393	0.0270	1.543	0.014	1.509	0.046	102
AH 1248	21.1	3.5092	0.0693	0.2757	0.0026	0.900	3.6269	0.0342	0.0923	0.0019	0.0866	0.0710	1.570	0.013	1.474	0.040	106
AH 1248	5.2	3.6181	0.0810	0.2776	0.0028	0.990	3.6028	0.0365	0.0945	0.0024	0.5054	0.1721	1.579	0.014	1.519	0.048	103
AH 1248	28.1	0.9198	0.0532	0.1075	0.0022	0.830	9.2985	0.1925	0.0620	0.0035	0.8023	0.1539	0.658	0.013	0.675	0.115	97
AH1248	1.1	2.0763	0.0932	0.1904	0.0021	0.960	5.2519	0.0585	0.0791	0.0038	0.4334	0.0841	1.124	0.012	1.174	0.112	95
AH 1248	22.1	2.1424	0.1203	0.1941	0.0039	0.880	5.1517	0.1023	0.0800	0.0046	0.1147	0.0517	1.144	0.021	1.198	0.116	95
AH 1248	17.1	3.3368	0.0652	0.2636	0.0024	0.360	3.7938	0.0338	0.0918	0.0019	0.1028	0.0516	1.508	0.012	1.464	0.041	103
AH 1248	19.1	0.5142	0.0127	0.0570	0.0006	0.970	17.5393	0.1870	0.0654	0.0016	0.0648	0.0146	0.357	0.004	0.787	0.050	45
AH 1248	23.1	0.5174	0.0347	0.0731	0.0017	0.950	13.6830	0.3264	0.0513	0.0031	0.3040	0.0414	0.455	0.010	0.256	0.137	177
AH 1248	1.2	1.4083	0.0938	0.1192	0.0029	0.980	8.3870	0.2073	0.0857	0.0061	0.5170	0.0834	0.726	0.017	1.331	0.143	54
AH 1248	24.1	1.4580	0.1039	0.1385	0.0034	0.980	7.2213	0.1787	0.0764	0.0047	0.2162	0.0689	0.836	0.019	1.105	0.121	75
AH 1248	15.2	1.5525	0.1207	0.1468	0.0039	0.980	6.8109	0.1802	0.0767	0.0049	0.3055	0.0364	0.883	0.021	1.113	0.121	79
AH 1248	17.2	1.7359	0.1106	0.1514	0.0035	0.800	6.6052	0.1532	0.0832	0.0051	0.1521	0.0408	0.909	0.020	1.273	0.118	71
AH 1248	20.1	1.2965	0.0383	0.1519	0.0018	0.840	6.5842	0.0797	0.0619	0.0018	0.1032	0.0416	0.911	0.010	0.671	0.066	135
AH 1248	25.1	1.7489	0.1193	0.1635	0.0041	0.960	6.1161	0.1524	0.0776	0.0045	0.1650	0.0220	0.976	0.022	1.136	0.113	85
AH 1248	14.1	2.2216	0.0452	0.1839	0.0017	0.850	5.4385	0.0509	0.0876	0.0019	0.3575	0.3714	1.088	0.009	1.374	0.042	79
AH 1248	12.1	2.1552	0.0542	0.1867	0.0022	0.940	5.3559	0.0621	0.0837	0.0018	0.1021	0.0150	1.104	0.011	1.286	0.042	85
AH 1248	26.1	2.1568	0.1129	0.1896	0.0036	0.980	5.2733	0.1006	0.0825	0.0047	0.1702	0.1228	1.119	0.020	1.257	0.121	89
AH 1248	13.1	2.3148	0.0510	0.1987	0.0020	0.660	5.0334	0.0496	0.0845	0.0018	0.1299	0.1006	1.168	0.010	1.304	0.041	89

Continue...

Annex I. Continuation.

Sample	Spot	Ratios											Ages				206/238
		207/235	1σ err	206/238	1σ err	coef. corr	238/206	1σ err	207/206	1σ err	208/206	1σ err	T206/238	1σ err	T207/206	1σ err	207/206
AH1248	4.1	1.9494	0.0847	0.2236	0.0022	0.970	4.4725	0.0447	0.0632	0.0026	0.0455	0.0077	1.301	0.012	0.716	0.086	181
AH 1248	29.1	2.2456	0.1414	0.2256	0.0051	0.910	4.4317	0.1005	0.0722	0.0041	0.3780	0.0620	1.312	0.027	0.991	0.114	132
AH1248	8.1	1.9075	0.0816	0.2336	0.0022	0.640	4.2804	0.0403	0.0592	0.0025	0.0976	0.0173	1.353	0.011	0.575	0.090	235
AH1248	11.1	2.5229	0.1108	0.2733	0.0026	0.010	3.6584	0.0353	0.0669	0.0029	0.1916	0.0352	1.558	0.013	0.836	0.092	186
AH1248	2.1	2.5165	0.1103	0.2735	0.0027	0.730	3.6559	0.0365	0.0667	0.0028	0.1505	0.0565	1.559	0.014	0.829	0.086	187
AH1248	5.1	3.1815	0.1670	0.2758	0.0033	0.960	3.6262	0.0438	0.0837	0.0043	0.2857	0.0410	1.570	0.017	1.285	0.098	122
AH1248	9.1	2.5528	0.1216	0.2867	0.0030	0.900	3.4876	0.0359	0.0646	0.0031	0.1155	0.0058	1.625	0.015	0.760	0.101	213
AH 1248	18.1	3.1811	0.0613	0.2885	0.0026	0.900	3.4667	0.0312	0.0800	0.0017	0.1760	0.0505	1.634	0.013	1.197	0.047	136
AH 1248	2.2	3.1259	0.1857	0.2899	0.0062	0.900	3.4491	0.0734	0.0782	0.0045	0.0696	0.0063	1.641	0.031	1.152	0.114	142
AH1248	10.1	3.1388	0.1773	0.2935	0.0037	0.930	3.4072	0.0433	0.0776	0.0045	0.3933	0.0790	1.659	0.019	1.136	0.116	146
AH1248	7.1	3.4501	0.1561	0.3032	0.0031	0.999	3.2984	0.0342	0.0825	0.0034	0.0330	0.0107	1.707	0.015	1.258	0.081	135
AH 1248	21.2	3.6313	0.2122	0.3031	0.0063	0.990	3.2990	0.0682	0.0869	0.0050	0.0730	0.0791	1.707	0.031	1.358	0.109	125
J42	1.2	4.7215	0.2119	0.3177	0.0037	0.999	3.1478	0.0369	0.1078	0.0044	0.0658	0.0037	1.778	0.018	1.762	0.075	100
J42	1.1	4.7981	0.2020	0.3188	0.0036	0.999	3.1372	0.0352	0.1092	0.0047	0.1133	0.0297	1.784	0.018	1.786	0.079	99
J 42	2.2	4.9001	0.1492	0.3219	0.0027	0.950	3.1070	0.0257	0.1104	0.0033	0.1864	0.0116	1.799	0.013	1.806	0.053	99
J 42	19.2	4.9645	0.1530	0.3335	0.0029	0.990	2.9982	0.0257	0.1080	0.0034	0.1387	0.0193	1.856	0.014	1.765	0.059	105
J 42	16.1	5.0756	0.1448	0.3423	0.0026	0.950	2.9215	0.0225	0.1075	0.0030	0.1556	0.0045	1.898	0.013	1.758	0.051	107
J 42	15.1	5.2269	0.1760	0.3427	0.0032	0.999	2.9181	0.0273	0.1106	0.0038	0.1667	0.0101	1.900	0.015	1.810	0.063	104
J42	2.1	5.2365	0.2422	0.3521	0.0045	0.930	2.8400	0.0361	0.1079	0.0048	0.1894	0.0056	1.945	0.021	1.764	0.083	110
J 42	14.1	5.0948	0.1527	0.3444	0.0028	0.980	2.9040	0.0239	0.1073	0.0034	0.1827	0.0391	1.908	0.014	1.754	0.060	108
J 42	20.1	5.2084	0.1483	0.3486	0.0027	0.840	2.8690	0.0221	0.1084	0.0031	0.1791	0.0053	1.928	0.013	1.772	0.052	108
J42	8.1i	1.0815	0.0465	0.1203	0.0013	0.980	8.3139	0.0915	0.0652	0.0026	0.1043	0.0034	0.732	0.008	0.781	0.084	93
J42	3.1	1.5682	0.0660	0.1514	0.0017	0.980	6.6067	0.0730	0.0751	0.0030	0.0578	0.0071	0.909	0.009	1.072	0.080	84
J42	5.1B	1.6932	0.0720	0.1646	0.0018	0.950	6.0746	0.0663	0.0746	0.0030	0.0536	0.0011	0.982	0.010	1.058	0.081	92
J42	9.1i	3.5188	0.1963	0.2674	0.0040	0.980	3.7392	0.0563	0.0954	0.0052	0.2362	0.0129	1.528	0.020	1.537	0.101	99
J 42	12.1	3.7369	0.1076	0.2911	0.0022	0.950	3.4353	0.0262	0.0931	0.0026	0.0687	0.0169	1.647	0.011	1.490	0.053	110
J 42	13.1	4.3371	0.1177	0.3066	0.0022	0.960	3.2620	0.0237	0.1026	0.0028	0.0695	0.0051	1.724	0.011	1.672	0.051	103
J42	4.1	2.4059	0.1514	0.1955	0.0031	0.990	5.1142	0.0798	0.0892	0.0044	0.1213	0.0137	1.151	0.016	1.409	0.087	81
J42	6.1f	2.2598	0.0894	0.2137	0.0022	0.999	4.6793	0.0483	0.0767	0.0030	0.0662	0.0018	1.249	0.012	1.113	0.080	112
J42	7.1	4.8574	0.2512	0.3504	0.0050	0.930	2.8539	0.0409	0.1005	0.0051	0.1647	0.0112	1.936	0.024	1.634	0.095	118
J42	10.1	4.3198	0.1957	0.3550	0.0042	0.980	2.8168	0.0334	0.0883	0.0039	0.1773	0.0525	1.958	0.020	1.388	0.087	141
J42	11.1	4.9637	0.2375	0.3736	0.0048	0.950	2.6764	0.0342	0.0964	0.0044	0.1423	0.0163	2.046	0.022	1.555	0.085	131
J 42	5.2	1.6510	0.0553	0.1796	0.0015	0.520	5.5693	0.0478	0.0667	0.0021	0.0603	0.0047	1.065	0.008	0.828	0.065	128
J 42	9.2	3.5614	0.1132	0.2454	0.0021	0.980	4.0751	0.0348	0.1053	0.0032	0.1070	0.0130	1.415	0.011	1.719	0.056	82
J 42	17.1	1.3116	0.0479	0.1250	0.0012	0.990	7.9969	0.0766	0.0761	0.0021	0.0431	0.0062	0.760	0.007	1.097	0.055	69
J 42	18.1	2.2789	0.0807	0.1821	0.0017	0.990	5.4906	0.0501	0.0907	0.0029	0.1747	0.0268	1.079	0.009	1.441	0.059	74

Continue...

Annex I. Continuation.

Sample	Spot	Ratios											Ages				206/238
		207/235	1σ err	206/238	1σ err	coef. corr	238/206	1σ err	207/206	1σ err	208/206	1σ err	T206/238	1σ err	T207/206	1σ err	207/206
J 42	19.1	3.3409	0.1108	0.2417	0.0021	0.980	4.1379	0.0366	0.1003	0.0032	0.1493	0.0138	1.395	0.011	1.629	0.059	85
J98	1.1	4.6414	0.2140	0.3165	0.0045	0.950	3.1600	0.0447	0.1064	0.0048	0.1761	0.0048	1.772	0.022	1.738	0.083	101
J98	20.1	4.7344	0.1428	0.3192	0.0031	0.940	3.1325	0.0305	0.1076	0.0033	0.1993	0.0051	1.786	0.015	1.758	0.055	101
J98	15.1	4.7204	0.1503	0.3206	0.0033	0.950	3.1188	0.0318	0.1068	0.0034	0.2588	0.0235	1.793	0.016	1.745	0.058	102
J98	6.1	4.7774	0.2197	0.3216	0.0047	0.900	3.1090	0.0451	0.1077	0.0050	0.1800	0.0084	1.798	0.023	1.761	0.086	102
J98	3.1	4.7700	0.2166	0.3219	0.0046	0.870	3.1069	0.0443	0.1075	0.0051	0.2797	0.0138	1.799	0.022	1.757	0.087	102
J98	19.1	4.8515	0.1454	0.3273	0.0032	0.950	3.0549	0.0295	0.1075	0.0033	0.2414	0.0117	1.826	0.015	1.757	0.056	103
J98	17.1	4.8812	0.1653	0.3326	0.0036	0.910	3.0062	0.0329	0.1064	0.0038	0.2180	0.0098	1.851	0.018	1.739	0.065	106
J98	12.1	4.9617	0.1536	0.3334	0.0033	0.980	2.9994	0.0301	0.1079	0.0034	0.2116	0.0091	1.855	0.016	1.765	0.059	105
J98	2.1	4.6519	0.2234	0.3073	0.0048	0.010	3.2544	0.0510	0.1098	0.0055	0.1979	0.0070	1.727	0.024	1.796	0.093	96
J98	16.1	5.0418	0.1603	0.3374	0.0035	0.880	2.9639	0.0305	0.1084	0.0036	0.2355	0.0150	1.874	0.017	1.772	0.060	105
J98	18.1	5.0217	0.1655	0.3426	0.0037	0.940	2.9189	0.0314	0.1063	0.0038	0.1707	0.0035	1.899	0.018	1.737	0.065	109
J98	11.1	5.2108	0.2332	0.3459	0.0050	0.880	2.8907	0.0420	0.1092	0.0052	0.1748	0.0103	1.915	0.024	1.787	0.087	107
J98	4.1	5.6694	0.2762	0.3953	0.0058	0.999	2.5300	0.0373	0.1040	0.0044	0.5236	0.1065	2.147	0.026	1.697	0.078	126
J98	8.1	3.6780	0.1635	0.2516	0.0034	0.890	3.9753	0.0537	0.1060	0.0047	0.2209	0.0181	1.446	0.018	1.732	0.081	83
J98	14.1	3.8352	0.1195	0.2594	0.0026	0.990	3.8547	0.0386	0.1072	0.0034	0.2576	0.0153	1.487	0.013	1.753	0.059	84
J98	7.1	3.9839	0.1919	0.2719	0.0042	0.980	3.6782	0.0571	0.1063	0.0056	0.2059	0.0054	1.550	0.021	1.737	0.097	89
J98	5.1	4.1932	0.1932	0.2810	0.0041	0.940	3.5583	0.0518	0.1082	0.0051	0.3019	0.0139	1.597	0.021	1.770	0.087	90
J98	21.1	4.3710	0.1312	0.2964	0.0029	0.999	3.3740	0.0327	0.1070	0.0034	0.2366	0.0161	1.673	0.014	1.748	0.059	95
J98	10.1	4.3906	0.1436	0.2975	0.0031	0.970	3.3618	0.0353	0.1071	0.0038	0.2017	0.0065	1.679	0.016	1.750	0.065	95
J98	13.1	4.4905	0.1754	0.3016	0.0038	0.290	3.3157	0.0418	0.1080	0.0045	0.3164	0.0163	1.699	0.019	1.766	0.076	96
J 159	5.1	4.8326	0.2042	0.3226	0.0032	0.850	3.0999	0.0307	0.1086	0.0045	0.1985	0.0313	1.802	0.016	1.777	0.078	101
J 159	12.3	4.8640	0.1167	0.3262	0.0026	0.890	3.0653	0.0247	0.1081	0.0025	0.0334	0.0187	1.820	0.013	1.768	0.042	102
J 159	7.1	5.0194	0.1403	0.3288	0.0033	0.990	3.0413	0.0303	0.1107	0.0032	0.2024	0.0189	1.833	0.016	1.811	0.052	101
J 159	1.1	5.0358	0.2466	0.3308	0.0038	0.710	3.0232	0.0351	0.1104	0.0052	0.2136	0.0362	1.842	0.018	1.806	0.084	101
J 159	14.1	4.9381	0.1271	0.3317	0.0030	0.810	3.0146	0.0269	0.1080	0.0028	0.1653	0.0130	1.847	0.014	1.765	0.047	104
J 159	19.1	4.9322	0.1247	0.3334	0.0029	0.950	2.9996	0.0258	0.1073	0.0026	0.1971	0.0126	1.855	0.014	1.754	0.045	105
J 159	15.1	5.0149	0.1350	0.3351	0.0032	0.880	2.9839	0.0286	0.1085	0.0030	0.1867	0.0513	1.863	0.015	1.775	0.050	104
J 159	16.1	4.9910	0.1375	0.3358	0.0032	0.960	2.9782	0.0288	0.1078	0.0030	0.2188	0.0139	1.866	0.016	1.763	0.050	105
J 159	18.1	5.0169	0.1540	0.3364	0.0037	0.470	2.9727	0.0331	0.1082	0.0035	0.1971	0.0071	1.869	0.018	1.769	0.059	105
J 159	21.1	5.0023	0.1344	0.3373	0.0032	0.920	2.9643	0.0279	0.1075	0.0028	0.2426	0.0268	1.874	0.015	1.758	0.048	106
J 159	22.1	5.0482	0.1606	0.3389	0.0040	0.920	2.9511	0.0344	0.1080	0.0036	0.2103	0.0079	1.881	0.019	1.767	0.061	106
J 159	17.1	5.1166	0.1355	0.3412	0.0032	0.940	2.9311	0.0276	0.1088	0.0030	0.2528	0.0196	1.892	0.016	1.779	0.051	106
J 159	20.1	5.1348	0.1382	0.3439	0.0033	0.880	2.9075	0.0275	0.1083	0.0029	0.2358	0.0063	1.906	0.016	1.771	0.050	107
J 159	12.1	5.1990	0.2197	0.3472	0.0033	0.850	2.8802	0.0272	0.1086	0.0044	0.1218	0.0147	1.921	0.016	1.776	0.074	108
J 159	13.1	5.2973	0.2405	0.3447	0.0037	0.860	2.9012	0.0313	0.1115	0.0050	0.1542	0.0175	1.909	0.018	1.823	0.083	104

Continue...

Annex I. Continuation.

Sample	Spot	Ratios											Ages				206/238
		207/235	1σ err	206/238	1σ err	coef. corr	238/206	1σ err	207/206	1σ err	208/206	1σ err	T206/238	1σ err	T207/206	1σ err	207/206
J 159	8.1	5.1945	0.2308	0.3460	0.0035	0.920	2.8904	0.0293	0.1089	0.0046	0.1722	0.0078	1.915	0.017	1.781	0.077	107
J 159	2.1	5.2970	0.2157	0.3468	0.0032	0.840	2.8833	0.0267	0.1108	0.0044	4.4055	25.6843	1.919	0.015	1.812	0.072	105
J 159	4.1	5.3876	0.2929	0.3488	0.0046	0.120	2.8670	0.0381	0.1120	0.0061	0.2355	0.0252	1.929	0.022	1.833	0.099	105
J 159	10.1	5.2967	0.2366	0.3518	0.0036	0.600	2.8423	0.0292	0.1092	0.0048	0.2657	0.0213	1.943	0.017	1.786	0.079	108
J 159	11.1	5.2603	0.2206	0.3520	0.0033	0.870	2.8406	0.0267	0.1084	0.0043	0.1110	0.0059	1.944	0.016	1.772	0.072	109
J 159	3.1	5.4434	0.2317	0.3559	0.0035	0.970	2.8098	0.0275	0.1109	0.0047	0.1961	0.0077	1.963	0.017	1.815	0.076	108
J 159	9.1	5.4885	0.2738	0.3597	0.0043	0.760	2.7802	0.0333	0.1107	0.0055	0.2012	0.0087	1.981	0.020	1.810	0.091	109
J 159	2.2	5.6415	0.1212	0.3723	0.0027	0.999	2.6857	0.0197	0.1099	0.0026	0.1642	0.0598	2.040	0.013	1.798	0.043	113
J 159	6.1	5.5019	0.2485	0.3634	0.0038	0.940	2.7521	0.0286	0.1098	0.0048	0.1624	0.0039	1.998	0.018	1.796	0.080	111
J 159	7.1	4.6764	0.2353	0.3053	0.0037	0.970	3.2752	0.0394	0.1111	0.0057	0.1356	0.0172	1.718	0.018	1.817	0.093	94
J 159	12.2	5.2594	0.1363	0.3482	0.0032	0.790	2.8718	0.0261	0.1095	0.0029	0.0944	0.0497	1.926	0.015	1.792	0.048	107
PR3228	9.1	0.9998	0.0568	0.0787	0.0018	0.990	12.7128	0.2885	0.0922	0.0052	0.1266	0.0147	0.488	0.011	1.471	0.107	33
PR3228	20.1	1.0403	0.0357	0.0853	0.0012	0.990	11.7205	0.1610	0.0884	0.0024	0.2415	0.0626	0.528	0.007	1.392	0.052	37
PR3228	27.1	1.0580	0.0270	0.0887	0.0008	0.990	11.2717	0.1025	0.0865	0.0022	0.1837	0.0307	0.548	0.005	1.349	0.049	40
PR3228	24.1	1.3841	0.0377	0.1064	0.0010	0.999	9.4017	0.0926	0.0944	0.0024	0.0815	0.0188	0.652	0.006	1.516	0.048	42
PR3228	2.2	1.4504	0.0405	0.1086	0.0011	0.999	9.2042	0.0908	0.0968	0.0030	0.2593	0.0257	0.665	0.006	1.564	0.059	42
PR3228	1.1	1.5898	0.0609	0.1159	0.0016	0.970	8.6248	0.1206	0.0994	0.0040	0.2283	0.0150	0.707	0.009	1.614	0.075	43
PR3228	7.1	1.7215	0.0683	0.1266	0.0018	0.630	7.8981	0.1103	0.0986	0.0040	0.1141	0.0215	0.769	0.010	1.598	0.074	48
PR3228	24.2	2.1287	0.0471	0.1626	0.0013	0.990	6.1484	0.0502	0.0949	0.0024	0.0819	0.0314	0.971	0.007	1.527	0.048	63
PR3228	15.1	2.2896	0.0527	0.1731	0.0014	0.999	5.7765	0.0471	0.0959	0.0024	0.1140	0.0251	1.029	0.008	1.546	0.047	66
PR3228	1.2	2.5180	0.0720	0.1795	0.0019	0.990	5.5713	0.0583	0.1017	0.0031	0.1877	0.0197	1.064	0.010	1.656	0.056	64
PR3228	12.2	2.5964	0.0744	0.1848	0.0021	0.999	5.4098	0.0601	0.1019	0.0028	0.1960	0.0075	1.093	0.011	1.659	0.051	65
PR3228	4.2	2.5545	0.0657	0.1850	0.0017	0.990	5.4068	0.0507	0.1002	0.0026	0.2197	0.0295	1.094	0.009	1.627	0.050	67
PR3228	21.1	2.9789	0.0796	0.2205	0.0023	0.999	4.5345	0.0468	0.0980	0.0026	0.2560	0.0552	1.285	0.012	1.586	0.050	81
PR3228	2.5	3.1696	0.1183	0.2273	0.0029	0.750	4.3992	0.0565	0.1011	0.0037	0.1791	0.0053	1.320	0.015	1.645	0.068	80
PR3228	4.1	3.4902	0.1380	0.2421	0.0036	0.950	4.1301	0.0610	0.1045	0.0042	0.2257	0.0062	1.398	0.019	1.706	0.075	81
PR3228	8.1	3.4189	0.1235	0.2464	0.0030	0.960	4.0585	0.0501	0.1006	0.0036	0.1690	0.0033	1.420	0.016	1.636	0.067	86
PR3228	12.1	3.6555	0.1447	0.2571	0.0038	0.780	3.8903	0.0576	0.1031	0.0042	0.1602	0.0066	1.475	0.020	1.681	0.075	87
PR3228	2.1	3.8671	0.1561	0.2680	0.0044	0.950	3.7316	0.0612	0.1047	0.0047	0.2507	0.0204	1.531	0.023	1.708	0.083	89
PR3228	29.1	3.7695	0.0768	0.2720	0.0021	0.999	3.6763	0.0280	0.1005	0.0025	0.1416	0.0055	1.551	0.011	1.633	0.048	94
PR3228	14.1	3.7014	0.0929	0.2760	0.0024	0.980	3.6236	0.0319	0.0973	0.0027	0.2171	0.1298	1.571	0.012	1.573	0.051	99
PR3228	11.1	4.0880	0.1581	0.2854	0.0041	0.920	3.5034	0.0500	0.1039	0.0041	0.2180	0.0116	1.619	0.020	1.694	0.072	95
PR3228	13.1	4.2934	0.1629	0.3002	0.0041	0.600	3.3308	0.0454	0.1037	0.0040	0.3139	0.0267	1.692	0.020	1.692	0.071	100
PR3228	3.2	4.3267	0.1097	0.3073	0.0027	0.990	3.2541	0.0289	0.1021	0.0026	0.1883	0.0165	1.727	0.013	1.663	0.046	103
PR3228	11.2	4.7007	0.1221	0.3252	0.0031	0.990	3.0748	0.0295	0.1048	0.0029	0.1846	0.0408	1.815	0.015	1.711	0.051	106

Continue...

Annex I. Continuation.

Sample	Spot	Ratios											Ages				206/238
		207/235	1σ err	206/238	1σ err	coef. corr	238/206	1σ err	207/206	1σ err	208/206	1σ err	T206/238	1σ err	T207/206	1σ err	207/206
PR3228	16.1	2.9286	0.0705	0.2320	0.0019	0.960	4.3104	0.0360	0.0916	0.0021	0.0387	0.0061	1.345	0.010	1.458	0.045	92
PR3228	18.1	3.2095	0.0843	0.2598	0.0022	0.980	3.8495	0.0329	0.0896	0.0022	1.6957	0.4373	1.489	0.011	1.417	0.045	105
PR3228	25.1	2.6141	0.0663	0.2190	0.0020	0.990	4.5657	0.0414	0.0866	0.0022	0.1867	0.0407	1.277	0.010	1.351	0.047	94
PR3228	6.1	0.7243	0.0267	0.0686	0.0009	0.990	14.5813	0.1837	0.0766	0.0029	0.3004	0.0249	0.428	0.005	1.111	0.077	38
PR3228	5.1	1.1994	0.0453	0.1026	0.0013	0.970	9.7436	0.1253	0.0848	0.0031	0.1262	0.0103	0.630	0.008	1.310	0.073	48
PR3228	13.2	1.6609	0.0653	0.1430	0.0020	0.980	6.9931	0.0980	0.0842	0.0025	0.2686	0.3766	0.862	0.011	1.298	0.052	66
PR3228	14.2	1.9140	0.0490	0.1578	0.0015	0.960	6.3356	0.0585	0.0879	0.0022	0.1662	0.0535	0.945	0.008	1.381	0.049	68
PR3228	17.1	2.1306	0.0529	0.1803	0.0015	0.860	5.5465	0.0475	0.0857	0.0021	0.1174	0.0155	1.069	0.008	1.332	0.048	80
PR3228	18.2	3.3986	0.0766	0.2817	0.0024	0.930	3.5494	0.0297	0.0875	0.0020	1.9408	0.1997	1.600	0.012	1.371	0.045	116
PR3228	19.1	1.0006	0.0437	0.1013	0.0015	0.990	9.8723	0.1434	0.0716	0.0021	0.6122	0.0945	0.622	0.008	0.976	0.051	63
PR3228	22.1	1.6197	0.0495	0.1391	0.0017	0.999	7.1872	0.0859	0.0844	0.0024	1.2693	0.4022	0.840	0.009	1.302	0.051	64
PR3228	23.1	2.8549	0.0699	0.2194	0.0019	0.980	4.5586	0.0400	0.0944	0.0022	0.1172	0.0054	1.279	0.010	1.516	0.044	84
PR3228	26.1	2.0026	0.0480	0.1772	0.0015	0.760	5.6433	0.0480	0.0820	0.0020	0.1688	0.0349	1.052	0.008	1.245	0.047	84
PR3228	28.1	2.0427	0.0451	0.1811	0.0014	0.970	5.5213	0.0436	0.0818	0.0019	0.1032	0.0100	1.073	0.008	1.241	0.046	86

Annex II. Isotope ratio data for samples analysed by SHRIMP method (errors are 1s unless otherwise specified).

Spot Name	ppm U	ppm Th	232Th /238U	ppm Rad 206Pb	204corr 206Pb /238U Age	1σ err	204corr 207Pb /206Pb Age	1σ err	% Disc	4corr 207r /206r	% err	4corr 207r /235	% err	4corr 206r /238	% err	Err corr
J36-1.1	373	120	0.33	64.6	1154.0	10.3	1637	61	42	.1007	3.3	2.72	3.4	.1960	1.0	.287
J36-2.1	186	70	0.39	28.0	1036.5	9.9	1047	31	1	.0742	1.5	1.78	1.9	.1744	1.0	.559
J36-3.1	235	98	0.43	56.3	1578.0	14.3	1580	23	0	.0977	1.2	3.73	1.6	.2773	1.0	.632
J36-4.1	230	111	0.50	76.0	2094.2	17.7	2197	8	5	.1376	0.4	7.28	1.1	.3838	1.0	.915
J36-5.1	404	393	1.00	73.9	1228.9	10.7	1543	32	26	.0958	1.7	2.77	2.0	.2100	1.0	.485
J36-6.1	284	197	0.72	74.0	1707.5	14.5	1757	8	3	.1075	0.5	4.49	1.1	.3033	1.0	.903
J36-7.1	287	20	0.07	76.3	1729.3	14.6	2005	13	16	.1233	0.8	5.23	1.2	.3077	1.0	.785
J36-8.1	578	136	0.24	172.2	1908.5	15.7	1651	16	-14	.1014	0.9	4.82	1.3	.3445	1.0	.745
J36-9.1	91	54	0.61	19.9	1455.1	14.6	1514	26	4	.0943	1.4	3.29	1.8	.2532	1.1	.638
J36-10.1	645	418	0.67	180.8	1820.5	15.6	1749	5	-4	.1070	0.3	4.81	1.0	.3263	1.0	.966
J36-11.1	1280	514	0.42	316.5	1546.0	14.2	1524	135	-1	.0948	7.2	3.54	7.2	.2710	1.0	.142
J36-12.1	309	247	0.83	66.8	1438.2	14.6	1700	47	18	.1042	2.5	3.59	2.8	.2499	1.1	.408
J36-13.1	603	236	0.40	198.5	2089.8	16.6	2553	4	22	.1696	0.2	8.95	1.0	.3829	0.9	.969
J127MIZ-1.1	167	124	0.77	45.0	1745.3	15.9	1786	21	2	.1092	1.2	4.68	1.6	.3109	1.0	.663
J127MIZ-1.2	368	83	0.23	105.5	1853.0	17.8	1752	12	-5	.1072	0.6	4.92	1.3	.3330	1.1	.862
J127MIZ-2.1	190	112	0.61	51.3	1755.9	15.2	1787	12	2	.1093	0.6	4.72	1.2	.3131	1.0	.838
J127MIZ-3.1	161	99	0.63	43.6	1754.5	15.5	1781	19	1	.1089	1.0	4.70	1.4	.3128	1.0	.700
J127MIZ-4.1	273	135	0.51	74.0	1768.4	16.3	1781	8	1	.1089	0.5	4.74	1.1	.3156	1.1	.918
J127MIZ-4.2	119	100	0.87	45.0	1997.6	30.5	1919	373	-4	.1175	20.8	5.89	20.9	.3633	1.8	.085
J127MIZ-5.1	136	147	1.12	36.6	1750.3	16.2	1780	15	2	.1089	0.8	4.68	1.4	.3119	1.1	.780
J127MIZ-6.1	140	75	0.55	36.4	1702.2	15.8	1785	14	5	.1091	0.8	4.55	1.3	.3022	1.1	.803
J127MIZ-7.1	188	139	0.77	51.2	1769.4	15.4	1787	14	1	.1093	0.8	4.76	1.3	.3158	1.0	.782
J127MIZ-8.1	132	90	0.71	35.6	1761.5	19.4	1772	12	1	.1084	0.7	4.70	1.4	.3142	1.3	.879
J127MIZ-9.1	152	88	0.60	41.7	1773.8	16.3	1783	32	0	.1090	1.8	4.76	2.1	.3167	1.0	.510
J127MIZ-10.1	220	142	0.67	44.6	1363.0	12.1	1730	14	27	.1059	0.7	3.44	1.2	.2354	1.0	.798
J127MIZ-11.1	149	91	0.63	39.9	1722.2	15.7	1746	39	1	.1068	2.1	4.51	2.4	.3062	1.0	.441
J127MIZ-12.1	184	123	0.69	48.8	1726.9	15.1	1771	17	3	.1083	0.9	4.59	1.4	.3072	1.0	.727
J127MIZ-13.1	115	86	0.77	31.7	1792.0	18.5	1778	14	-1	.1087	0.8	4.80	1.4	.3205	1.2	.838
J127MIZ-14.1	211	199	0.98	55.9	1721.4	14.9	1757	22	2	.1075	1.2	4.54	1.5	.3061	1.0	.638
PR-3141M-2.1	230	165	0.74	50.5	1463.0	12.9	1506	19	3	.0939	1.0	3.30	1.4	.2548	1.0	.702
PR-3141M-3.1	933	258	0.29	194.0	1395.7	11.6	1485	9	6	.0928	0.5	3.09	1.0	.2417	0.9	.897
PR-3141M-4.1	232	284	1.27	43.0	1178.0	12.5	1464	188	24	.0918	9.9	2.54	9.9	.2005	1.2	.116
PR-3141M-5.1	140	130	0.96	31.0	1434.6	13.8	1483	78	3	.0928	4.1	3.19	4.2	.2492	1.1	.253
PR-3141M-6.1	143	124	0.89	33.1	1509.7	14.5	1493	53	-1	.0932	2.8	3.39	3.0	.2639	1.1	.362
PR-3141M-7.1	333	185	0.57	94.0	1820.1	15.7	1550	25	-15	.0961	1.3	4.32	1.7	.3262	1.0	.600
PR-3141M-8.1	175	185	1.09	38.8	1475.1	13.6	1504	15	2	.0938	0.8	3.33	1.3	.2571	1.0	.792

Continue...

Annex II. Continuation.

Spot Name	ppm U	ppm Th	232Th /238U	ppm Rad 206Pb	204corr 206Pb /238U Age	1σ err	204corr 207Pb /206Pb Age	1σ err	% Disc	4corr 207r /206r	% err	4corr 207r /235	% err	4corr 206r /238	% err	Err corr
PR-3141M-9.1	262	206	0.81	54.2	1384.0	12.2	1500	19	8	.0936	1.0	3.09	1.4	.2395	1.0	.690
PR-3141M-10.1	295	199	0.70	64.8	1454.1	12.6	1507	31	4	.0940	1.6	3.28	1.9	.2530	1.0	.511
PR-3141M-11.1	131	134	1.06	29.6	1500.9	13.9	1513	19	1	.0943	1.0	3.41	1.5	.2622	1.0	.713
PR-3141M-12.1	143	156	1.13	32.4	1507.7	13.9	1507	16	0	.0939	0.8	3.41	1.3	.2635	1.0	.780
PR-3141M-13.1	234	227	1.00	52.0	1484.5	13.0	1519	10	2	.0945	0.5	3.38	1.1	.2589	1.0	.881
PR-3141M-14.1	226	159	0.73	38.8	1151.4	10.7	1482	55	29	.0927	2.9	2.50	3.1	.1956	1.0	.329
PR-3141M-15.1	288	220	0.79	62.3	1441.6	12.7	1473	26	2	.0923	1.4	3.19	1.7	.2506	1.0	.578
EP2MI-1.1	128	82	0.67	33.3	1707.8	15.7	1738	15	2	.1063	0.8	4.45	1.3	.3033	1.0	.782
EP2MI-2.1	202	93	0.47	48.9	1595.7	14.1	1686	17	6	.1034	0.9	4.00	1.3	.2809	1.0	.741
EP2MI-3.1	620	334	0.56	106.3	1139.5	11.4	1632	68	43	.1004	3.7	2.68	3.8	.1934	1.1	.285
EP2MI-4.1	159	86	0.56	41.5	1697.1	21.7	1677	46	-1	.1029	2.5	4.27	2.9	.3012	1.5	.506
EP2MI-5.1	159	86	0.56	21.2	923.4	8.6	1677	46	82	.1029	2.5	2.18	2.7	.1540	1.0	.373
EP2MI-6.1	586	245	0.43	106.1	1194.6	10.7	1624	76	36	.1000	4.1	2.81	4.2	.2036	1.0	.234
EP2MI-7.1	137	253	1.91	35.1	1683.6	15.3	1715	16	2	.1050	0.9	4.32	1.3	.2984	1.0	.771
EP2MI-8.1	343	198	0.60	89.8	1713.7	14.4	1725	8	1	.1056	0.5	4.43	1.1	.3045	1.0	.904
EP2MI-9.1	279	149	0.55	72.2	1697.8	14.5	1725	10	2	.1056	0.5	4.39	1.1	.3013	1.0	.876
EP2MI-10.1	339	182	0.55	88.2	1702.7	14.3	1721	8	1	.1054	0.4	4.39	1.0	.3023	1.0	.912
EP2MI-11.1	410	239	0.60	98.8	1589.1	13.3	1707	11	7	.1046	0.6	4.03	1.1	.2796	0.9	.841
EP2MI-12.1	592	417	0.73	126.3	1403.2	11.9	1655	44	18	.1017	2.4	3.41	2.6	.2432	0.9	.370
EP2MI-13.1	140	70	0.51	40.2	1861.2	19.1	1742	15	-6	.1066	0.8	4.92	1.4	.3347	1.2	.815
EP2MI-14.1	417	327	0.81	106.9	1682.5	14.2	1717	8	2	.1052	0.4	4.32	1.0	.2982	1.0	.913
EP2MI-15.1	272	288	1.09	70.4	1694.3	14.7	1747	9	3	.1069	0.5	4.43	1.1	.3006	1.0	.886
EP2MI-16.1	254	110	0.45	75.8	1925.1	17.4	1756	11	-9	.1074	0.6	5.15	1.2	.3480	1.0	.869
J-84-1.1	326	436	1.38	56.7	1186.7	41.0	1458	14	23	.0916	0.7	2.55	3.9	.2021	3.8	.981
J-84-2.1	770	224	0.30	168.4	1462.9	49.4	1520	6	4	.0946	0.3	3.32	3.8	.2547	3.8	.997
J-84-3.1	171	155	0.94	41.7	1606.7	54.1	1963	19	22	.1204	1.1	4.70	3.9	.2830	3.8	.962
J-84-3.2	1978	754	0.39	288.9	1003.2	35.0	1411	26	41	.0893	1.4	2.07	4.0	.1684	3.8	.941
J-84-4.1	345	149	0.44	67.5	1320.3	45.2	1504	15	14	.0938	0.8	2.94	3.9	.2273	3.8	.980
J-84-6.1	227	113	0.51	23.3	722.2	26.2	1539	57	113	.0956	3.0	1.56	4.9	.1185	3.8	.785
J-84-7.1	550	163	0.31	89.1	1110.4	38.5	1533	16	38	.0952	0.8	2.47	3.9	.1880	3.8	.977
J-84-8.1	729	186	0.26	155.0	1378.4	49.6	1541	161	12	.0956	8.5	3.14	9.4	.2384	4.0	.423
J-84-9.1	194	141	0.75	42.0	1438.6	49.9	1455	31	1	.0914	1.6	3.15	4.2	.2500	3.9	.922
J-84-10.1	125	219	1.81	21.1	1116.0	39.2	1446	108	30	.0910	5.7	2.37	6.8	.1890	3.8	.559
J-84-1.2	120	195	1.68	26.6	1461.0	49.9	1480	59	1	.0926	3.1	3.25	4.9	.2544	3.8	.775
J-84-11.1	395	171	0.45	83.3	1409.9	47.8	1506	14	7	.0939	0.7	3.16	3.8	.2445	3.8	.981
PR-3001-1.1	291	77	0.27	75.5	1700.5	57.3	1740	8	2	.1065	0.4	4.43	3.9	.3019	3.8	.994

Continue...

Annex II. Continuation.

Spot Name	ppm U	ppm Th	232Th /238U	ppm Rad 206Pb	204corr 206Pb /238U Age	1σ err	204corr 207Pb /206Pb Age	1σ err	% Disc	4corr 207r /206r	% err	4corr 207r /235	% err	4corr 206r /238	% err	Err corr
PR-3001-2.1	316	91	0.30	77.9	1614.0	54.4	1708	20	6	.1047	1.1	4.11	4.0	.2845	3.8	.963
PR-3001-3.1	174	68	0.40	46.8	1756.0	58.3	1829	12	4	.1118	0.7	4.83	3.8	.3131	3.8	.986
PR-3001-4.1	467	445	0.98	120.0	1682.3	55.9	1762	10	5	.1078	0.5	4.43	3.8	.2982	3.8	.990
PR-3001-5.1	395	171	0.45	64.4	1115.4	38.7	1506	14	35	.0939	0.7	2.45	3.8	.1889	3.8	.981
PR-3001-6.1	309	64	0.21	62.4	1309.1	44.9	1696	97	30	.1040	5.3	3.23	6.5	.2252	3.8	.585
PR-3001-7.1	171	99	0.60	43.8	1670.9	55.8	1757	21	5	.1074	1.2	4.38	4.0	.2959	3.8	.956
PR-3001-8.1	346	115	0.34	88.6	1665.8	55.4	1734	25	4	.1061	1.3	4.31	4.0	.2949	3.8	.942
PR-3001-9.1	292	73	0.26	77.4	1727.5	57.2	1742	11	1	.1066	0.6	4.52	3.8	.3073	3.8	.987
PR-3001-10.1	564	224	0.41	154.7	1782.3	58.7	1739	10	-2	.1064	0.6	4.67	3.8	.3185	3.8	.989
PR-3001-11.1	1351	401	0.31	319.1	1548.4	51.8	1704	25	10	.1044	1.4	3.91	4.0	.2715	3.8	.941
PR-3001-12.1	607	125	0.21	144.8	1572.2	52.6	1712	13	9	.1049	0.7	3.99	3.8	.2762	3.8	.983
J-199-1.1	537	250	0.48	138.8	1691.0	56.2	1784	10	5	.1091	0.6	4.51	3.8	.2999	3.8	.989
J-199-2.1	309	161	0.54	80.9	1715.2	57.4	1785	9	4	.1091	0.5	4.59	3.8	.3048	3.8	.992
J-199-3.1	276	151	0.56	71.2	1687.6	56.7	1784	11	6	.1091	0.6	4.50	3.9	.2992	3.8	.989
J-199-4.1	439	166	0.39	113.5	1694.3	57.5	1805	7	7	.1103	0.4	4.57	3.9	.3006	3.9	.995
J-199-5.1	300	137	0.47	83.6	1801.0	59.3	1783	16	-1	.1090	0.9	4.84	3.9	.3223	3.8	.975
J-199-6.1	252	108	0.44	71.9	1847.3	60.8	1811	9	-2	.1107	0.5	5.06	3.8	.3318	3.8	.992
J-199-7.1	332	179	0.56	93.7	1797.2	59.3	1807	43	1	.1104	2.4	4.90	4.5	.3215	3.8	.846
J-199-8.1	415	198	0.49	117.6	1839.4	60.4	1802	6	-2	.1102	0.3	5.02	3.8	.3302	3.8	.996
J-199-9.1	269	133	0.51	76.9	1851.1	60.8	1812	7	-2	.1108	0.4	5.08	3.8	.3326	3.8	.994
J-199-10.1	257	120	0.48	72.1	1824.2	60.0	1797	8	-1	.1099	0.4	4.95	3.8	.3271	3.8	.993
J-199-11.1	410	181	0.46	115.9	1833.1	60.2	1790	6	-2	.1094	0.3	4.96	3.8	.3289	3.8	.996
J-199-12.1	533	346	0.67	150.5	1812.5	59.6	1786	27	-1	.1092	1.5	4.89	4.0	.3247	3.8	.931
HB-667-1.1	294	144	0.50	80.5	1782.9	58.9	1770	16	-1	.1083	0.9	4.76	3.9	.3186	3.8	.975
HB-667-1.2	299	109	0.38	76.2	1672.6	55.7	1775	10	6	.1085	0.5	4.43	3.8	.2962	3.8	.990
HB-667-2.1	2075	1012	0.50	311.6	1027.9	35.8	1461	28	42	.0917	1.5	2.19	4.0	.1729	3.8	.931
HB-667-3.1	340	247	0.75	85.7	1590.0	53.6	1761	105	11	.1077	5.7	4.15	6.9	.2797	3.8	.553
HB-667-4.1	368	154	0.43	100.4	1777.7	58.7	1767	7	-1	.1081	0.4	4.73	3.8	.3175	3.8	.995
HB-667-5.1	425	170	0.41	117.5	1799.5	59.2	1788	6	-1	.1093	0.3	4.85	3.8	.3220	3.8	.996
HB-667-6.1	955	468	0.51	264.6	1802.6	59.2	1761	4	-2	.1077	0.2	4.79	3.8	.3226	3.8	.998
HB-667-6.2	222	162	0.75	61.4	1798.4	59.3	1790	8	0	.1094	0.5	4.85	3.8	.3218	3.8	.993
HB-667-7.1	257	109	0.44	71.2	1803.2	59.4	1773	8	-2	.1084	0.4	4.83	3.8	.3228	3.8	.994
HB-667-8.1	400	254	0.66	110.3	1796.8	59.2	1778	6	-1	.1087	0.3	4.82	3.8	.3215	3.8	.996
HB-667-9.1	341	137	0.42	96.1	1830.5	60.2	1801	12	-2	.1101	0.7	4.99	3.8	.3284	3.8	.984
HB-667-10.1	470	407	0.89	130.0	1799.1	59.2	1774	6	-1	.1085	0.3	4.82	3.8	.3219	3.8	.997